

RESEARCH ARTICLE

Indices for daily temperature and precipitation in Madagascar, based on quality-controlled and homogenized data, 1950–2018

Luc Yannick Andréas Randriamarolaza^{1,2}  | Enric Aguilar¹  |
Oleg Skrynyk^{1,3}  | Sergio M. Vicente-Serrano⁴  | Fernando Domínguez-Castro^{5,6} 

¹Center for Climate Change (C3), Geography Department, Universitat Rovira i Virgili, Tarragona, Spain

²Direction de la Météorologie Appliquée, Direction Générale de la Météorologie, Antananarivo, Madagascar

³Division of Atmospheric Physics, Ukrainian Hydrometeorological Institute, Kyiv, Ukraine

⁴Instituto Pirenaico de Ecología, Spanish National Research Council (IPE-CSIC), Zaragoza, Spain

⁵Department of Geography, University of Zaragoza, Zaragoza, Spain

⁶ARAID Foundation, Zaragoza, Spain

Correspondence

Luc Yannick Andréas Randriamarolaza, 15 C. Joanot Martorell, Vila-seca, 43480, Spain.

Email: lucyannickandreas.randriamarolaza@urv.cat; luc.randriamarolaza@gmail.com

Funding information

FORMAS (SE), DLR (DE), BMWFW (AT), IFD (DK), MINECO (ES), ANR (FR), European Union, Grant/Award Number: 690462

Abstract

This study updates knowledge on climate evolution in Madagascar from 1950 to 2018. Changes were analyzed using annual and seasonal climate indices at regional and station level. The original daily series of minimum and maximum temperature and precipitation obtained from 28 meteorological stations were quality controlled and homogenized. Thirty-seven (37) climate indices were obtained from the daily series. The results show that changes in temperature had a higher degree of spatial coherence than changes in precipitation. Trends for temperature indices were mostly significant at 0.05 level and compatible with warming. Changes in minimum temperatures were greater than those for the maximum, leading to a significant decrease in the diurnal temperature range (DTR). Warm nights increased more than warm days, (0.70 days-decade⁻¹) and cold nights decreased more than cold days, (0.21 days-decade⁻¹). In addition, we found more stations with significant trends for very cold nights (92.60%) than for very warm days (51.80%) but they progressed differently (decrease and increase, respectively). Station-by-station precipitation index trends were mostly non-significant at 0.05 level, and most regional precipitation index showed decreasing trends. A shift in precipitation magnitude was observed around 2000–2018, a period of intensified drying (where 70.40% of stations recorded non-significant decreasing trends). An analysis of drought characteristics (i.e., intensity, magnitude and duration) highlighted the situation, especially in the south-east at an annual timescale.

KEYWORDS

climate change, climate indices, climate trends, Climatol, ClimInd, daily homogenization, HOMER, INQC, quality control

This is an open access article under the terms of the Creative Commons Attribution-NonCommercial-NoDerivs License, which permits use and distribution in any medium, provided the original work is properly cited, the use is non-commercial and no modifications or adaptations are made.

© 2021 The Authors. *International Journal of Climatology* published by John Wiley & Sons Ltd on behalf of Royal Meteorological Society.

1 | INTRODUCTION

The expert team on climate change detection and indices (ETCCDI) developed different indices to assess and monitor trends on climate extremes. Some of these indices are globally comparable and mostly based on tails of the distribution of meteorological variables, (Zhang *et al.*, 2011). Globally, changes in daily minimum temperature indices were faster than for daily maximum temperatures, and more heavy precipitation events were observed, as stated in Dunn *et al.* (2020).

In Africa, a first indices analysis indicated that cold and warm events decreased from 1960 to 1990 (Easterling *et al.*, 2003). These first findings were improved by introducing climate data quality control and homogenization processes. Therefore, more recent papers showed that cold and warm events were decreasing and increasing respectively for Southern and West Africa (New *et al.*, 2006), Western and Central Africa (Aguilar *et al.*, 2009) and the Western Indian Ocean Region (Vincent *et al.*, 2011). Also, Barry *et al.* (2018), using an updated data set, found that warm extremes were increasing and cold extremes decreasing in West Africa. In addition, homogenization improved coherency in the mean temperature trends among stations in South Africa (Kruger and Nxumalo, 2017).

In Madagascar, Tadross *et al.* (2008) and Vincent *et al.* (2011) agreed that annual temperature means increased from 1961 to 2005 and 1961 to 2008, respectively. However, certain inconsistencies were found for specific meteorological stations.

This study updates our understanding on how climate has changed in Madagascar. In comparison to the studies mentioned above, we extended the data period to 1950–2018 and used newly quality-controlled and homogenized data, including an assessment based on several climate indices. This assessment is highly relevant given climate change projections in the region. Nematchoua *et al.* (2018) suggested that warming could increase by more than 2°C, compared with 1960–2000, over the next decade in Madagascar based on A2 scenarios. According to Hoegh-Guldberg *et al.* (2018), 1.5°C above pre-industrial levels of global warming will be accompanied by larger temperature extremes and increased intensity and frequency of heavy precipitation and drought. For this reason, checking whether some of these projected changes could already be recorded in the observational data sets was a priority. For this purpose, we use a set of 28 quality controlled and homogenized stations (see Section 3 for details) and compute over them a set of 37 indices (see Domínguez-Castro *et al.* 2020), which extend the traditional set of ETCCDI indicators, to provide a complete assessment of the recent climate trends in Madagascar. Therefore, objectives of this study are to present

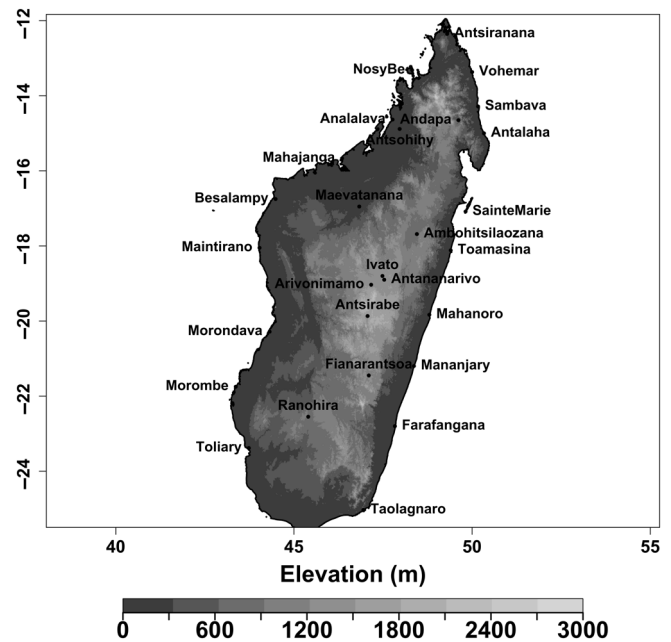


FIGURE 1 Relief and synoptic stations map of Madagascar. Elevation data are obtained from the SRTM digital elevation data in Jarvis *et al.* (Jarvis *et al.*, 2008)

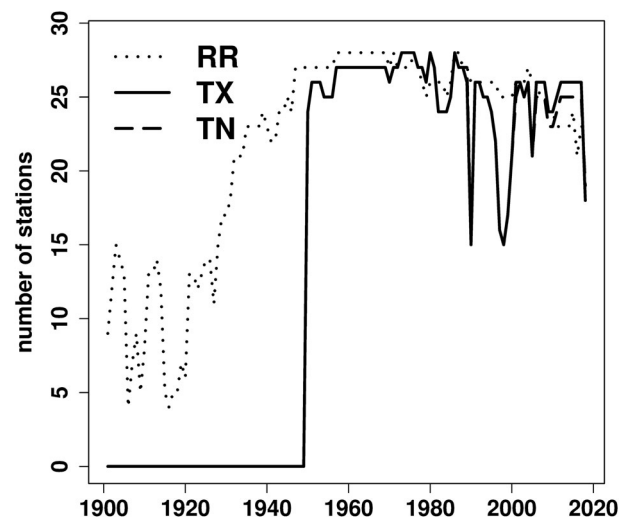


FIGURE 2 Number of synoptic weather stations per parameters. RR, precipitation; TX, maximum temperature; TN, minimum temperature

trends in observational indices on daily temperature and precipitation and analyze drought intensity, magnitude and duration in Madagascar over 1950–2018.

2 | STUDY AREA

Madagascar is located in the Western Indian Ocean, situated between latitudes 12°–25°S and longitudes

TABLE 1 Synoptic weather stations list

Stations	Longitude	Latitude	Elevation	WMO numbers	Start	End	Percentage of daily gaps		
							RR	TX	TN
Ambohitsilaozana	48.5	-17.7	786	67067	1928	2018	0.3	2.9	1.6
Analalava	47.8	-14.6	57	67019	1901	2017	26	15.5	32.6
Andapa ^a	49.6	-14.7	474	67022	1935	2008	52.7	51.4	51.6
Antalaha	50.3	-15.0	6	67025	1905	2018	0.2	18.9	18.7
Antananarivo	47.5	-18.9	1,310	67085	1943	2018	1.1	0.3	0.4
Antsirabe	47.1	-19.9	1,540	67107	1957	2018	2.8	9.2	8.7
Antsiranana	49.3	-12.4	105	67009	1901	2018	0.1	1.5	1.5
Antsohihy ^b	48.0	-14.9	28	67020	1923	2018	14.5	60.2	57.8
Arivonimamo ^a	47.2	-19.0	1,450	67109	1950	1981	100	54.2	54.2
Besalampy	44.5	-16.8	36	67037	1928	2018	2.2	17.1	15.9
Farafangana	47.8	-22.8	6	67157	1902	2018	0.7	7.1	8.4
Fianarantsoa	47.1	-21.5	1,106	67137	1902	2018	0	0.8	0.8
Ivato	47.5	-18.8	1,264	67083	1947	2018	0.4	0.5	0.5
Maevatanana ^b	46.8	-17.0	77	67045	1901	2017	17.3	40.5	40.5
Mahajanga	46.4	-15.7	22	67027	1897	2018	0	0.1	0.1
Mahanoro ^b	48.8	-19.8	5	67113	1903	2018	13.7	9.1	8.9
Maintirano	44.0	-18.1	25	67073	1903	2018	5.3	21.3	21.2
Mananjary	48.4	-21.2	6	67143	1901	2018	1.3	16.7	15.1
Morombe ^b	43.4	-21.8	4	67131	1928	2018	0.9	24.5	24.4
Morondava	44.3	-20.3	8	67117	1902	2018	3.3	4.8	4.2
NosyBe	48.3	-13.3	11	67012	1901	2018	6.7	7.8	7.7
Ranohira ^b	45.4	-22.6	823	67152	1935	2018	0.2	11.2	11.2
SainteMarie ^b	49.8	-17.1	9	67072	1947	2018	0.5	15.4	15.8
Sambava	50.2	-14.3	5	67023	1932	2018	1.8	14.5	15.2
Taolagnaro	47.0	-25.0	8	67197	1903	2018	0.5	0.6	0.7
Toamasina	49.4	-18.1	6	67095	1898	2018	0.7	7.3	6
Toliary	43.7	-23.4	9	67161	1901	2019	2	2.4	1.8
Voahemary ^b	50.0	-13.4	5	67017	1901	2017	19.5	15	14.7

Note: The longitude and latitude expressed in degrees and tenths of degree. Negative latitude corresponds to the southern, and longitude to the western, hemispheres. The percentages of valid values were calculated over period 1950–2018.

^aRemoved from analysis due to shorter records.

^bNot used by HOMER.

TABLE 2 Station relocation records

WMO numbers	Name	Station relocation	Reasons
67085	Antananarivo	March 1, 1953	Moved to Betongolo
67143	Mananjary	March 12, 1953	Moved to airport
67117	Morondava	October 1, 1955	Moved to airport
67197	Taolagnaro	February 20, 1953	Moved to airport
67161	Toliary	August 1955	Moved to airport

43°–51°E, and a surface area covering ~590,000 km². The climate is conditioned by its geographical position, relief, the maritime influence and wind regime, which is mainly

the easterly trade winds. Figure 1 shows the relief of Madagascar and the location of the available meteorological stations. The high mountains, running from north to

	TX	TN	RR	Total
Checked values	892	205	85	1,182
Validated	35	11	4	50
Corrected	201	194	6	401
Set to missing	656	0	75	731
Total values passing QC	704,764	705,451	705,571	2,115,786
Total raw values	705,656	705,656	705,656	2,116,968

TABLE 3 Summary of QC process

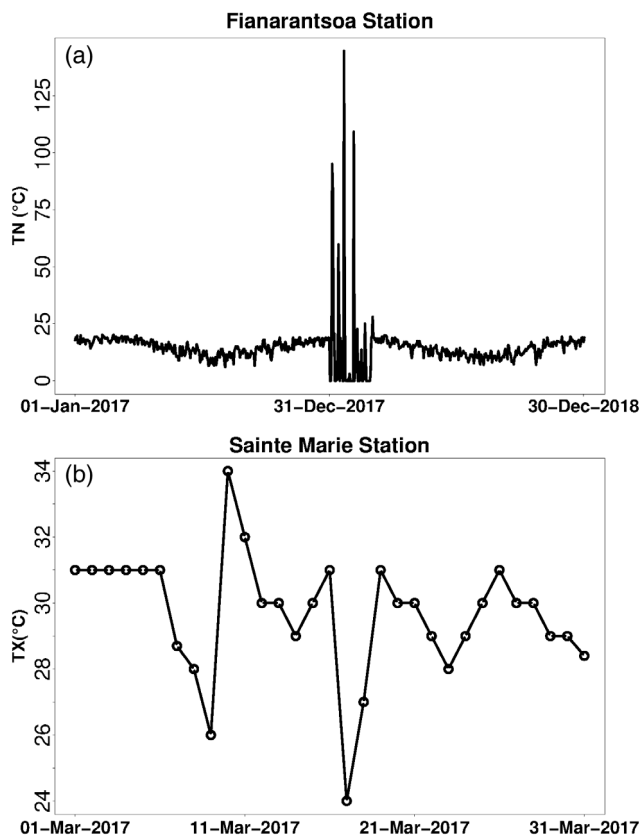


FIGURE 3 Examples of error types in raw data (a) erroneous and (b) suspects and collectively suspects

south, make the east and west as windward and leeward coasts respectively. Therefore, the west coast temperature is 1 to 3°C higher than on the east coast, but the east coast is wetter. The climate is clearly separated into two main seasons: wet and hot from November to April, and dry and cool from May to October. Mean annual temperature varies from 14 to 22°C in the highlands, and from 23 to 27°C in coastal areas. The lowest temperature occurs in July in the highlands, and the highest in November on the west coast. Their values are lower than 5°C and higher than 36°C respectively. The total annual rainfall varies from 350 mm on the south-west coast to 4,000 mm in the bay of Antongil (east coast).

During the hot, wet season, the easterly trade wind weakens but converges with the north-west monsoon wind to form the Inter-Tropical Convergence Zone (ITCZ), which covers the northern half of Madagascar. The analysis of annual zonal mean maximum precipitation and sea surface temperature done by Keshtgar *et al.* (2020) in Indian Ocean indicated that annual mean location of ITCZ was approximately 5.5°S. Moreover, Keshtgar *et al.* (2020) indicated also that the farthest south seasonal mean location of ITCZ was observed during December–January–February (DJF) and was approximately 7.5, 10.5 and 11.5°S according to analysis of seasonal zonal mean precipitation, mean wind speed near equator and zonal mean meridional wind respectively. Besides, Jury *et al.* (1994) found that ITCZ moved polewards to 15°S during DJF by analyzing outgoing longwave radiation. For instance, Randriamahefasoa and Reason (2017) noticed that this shift to southward of ITCZ associated to ENSO events influenced on the wet day frequency (daily rain exceeds 1 mm) in South and South-west regions. In addition, wet spells of these regions were also influenced by the development of tropical temperate trough (TTT) over Southern Africa and Mozambique channel from November to February as lined up by Macron *et al.* (2016). Ratna *et al.* (2013) showed that the TTT also modified the ITCZ structures. On the other hand, Donque (1972) remarked on the existence of a Mozambique Channel Trough (MCT) during this season. Then Barimalala *et al.* (2020) demonstrated that MCT appeared in December, intensified in February and weakened in May. Moreover, they concluded that a weak MCT activity caused dry conditions in Madagascar. Besides, the strong MCT activity promoted a cyclonic circulation over Mozambique channel (Barimalala *et al.*, 2020). Tropical cyclones (TCs) are frequent during this season. Madagascar is included in Southwest Indian Ocean basin (SWIO). It is boarded by Indian Ocean to the East and the Mozambique channel to the West. In SWIO, the frequency and tracks of (TCs) were related to ITCZ intensity and structure (Jury *et al.*, 1994). Jessica *et al.* (2016) ascertained that TCs period spanned from

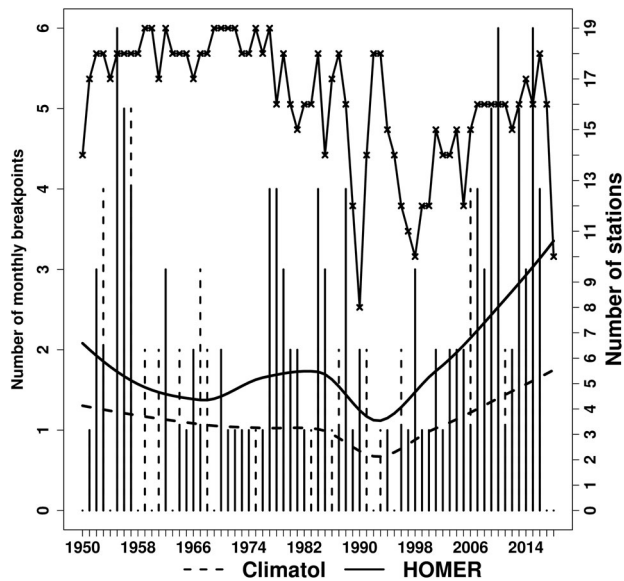


FIGURE 4 Comparison between number of monthly breakpoints for temperature for HOMER (line) and Climatol (dash) versus number of stations (cross). Number of stations was calculated from quality-controlled data such as data availability over the reference period 1961–1990 was 90% and no missing values more than 15 days in a year to calculate annual mean. The adjustment curves were done by LOESS function

November to April and its maximum activities were during DJF. On average, 9.7 tropical systems occurred of which around 97% (i.e., 9.4 up 9.7 on average) strengthened to tropical storms from which around 51% (i.e., 4.8 up 9.4 on average) became tropical cyclones (i.e., similar as hurricane or typhoon) each year during November to April as pointed out by Leroux *et al.* (2018). Besides, tropical activity and number of TC days were influenced by Indian Ocean Dipole (IOD) and El-Niño Southern Oscillation (ENSO) according to Jessica *et al.* (2016). Besides, Matyas (2015) showed that tropical cyclones formed in northern (southern) of Mozambique channel part if Indian Ocean Subtropical Dipole and Southern Annular Mode were negative (positive) phase. During the dry, cool season, the easterly trade wind dominates the island as noted by Donque (1972), who classified Madagascar into five climatic regions. Most regions receive rainfall during the hot, wet season, but the east coast continues to get rain even during the dry, cool season.

The eastern regions (reference stations: Vohemar, Sambava, Andapa, Antalaha, Sainte Marie, Ambohitsilaozana, Toamasina, Mahanoro, Mananjary, Farafangana, Taolaganro) are the most humid and threatened by tropical cyclones from the Indian Ocean. They receive around 2,500 mm per year and mean annual temperature is below 25°C. The central regions (reference stations: Ivato, Antananarivo, Arivonimamo,

Antsirabe, Fianarantsoa, Ranohira) are dominated by altitude climate. The mean annual temperature is around 20°C, and total annual rainfall around 1,200 mm. The western regions (reference stations: Analalava, Antsohihy, Mahajanga, Maevatanana, Besalampy, Maintiarano, Morondava, Morombe) are dry due to the foehn effect, although these regions receive rainfall when the ITCZ and Mozambique channel depression are well established. Annual rainfall is ~1,000 mm and mean annual temperature is above 25°C. The south and south-west regions (reference stations: Toliary) are dominated by a semi-arid climate. Annual rainfall is roughly 500 mm and mean annual temperature is around 23°C. The extreme north and north-west regions (reference stations: Antsiranana, Nosy-be) receive almost the same quantity of rainfall as in eastern regions, but the dry period is well-defined. The spatial pattern of rainfall is more discontinuous than temperature specifically in the south-western (dry area), where a single extreme rainfall can contribute a significant proportion of the annual rainfall (Tadross *et al.*, 2008).

3 | DATA AND METHODOLOGY

3.1 | Data

Daily minimum and maximum temperature and daily precipitation data measured at 28 synoptic stations were taken from the Directorate General of Meteorology (DGM) of Madagascar. Most of the stations are in coastal areas (Figure 1). Although the DGM stores some data prior to 1950, 1950–2018 are taken as the study period due to the high proportion of non-missing values at all stations (see Figure 2, Table 1). Metadata information, in addition to basic locational aspects, is very limited and we are only aware of the different station relocations listed in Table 2.

3.1.1 | Data quality control

Quality control (QC) is necessary to improve the accuracy of observations by detecting and identifying errors in the process of recording, manipulating, formatting, transmitting and archiving data (Aguilar *et al.*, 2003; WMO, 2020). For this purpose, we applied INQC, a new software developed by the authors within the framework of the INDECIS project (see <https://cran.r-project.org/web/packages/INQC/index.html>). INQC can be applied to quality control temperature, precipitation, relative humidity, wind speed, atmospheric pressure, snow depth, sunshine duration and cloud cover, and it was tested

TABLE 4 Annual and seasonal regional average trends and the confidence interval (in brackets) for temperature ($^{\circ}\text{C}/10$ years) and precipitation ($\%/10$ years) per method

Parameters	Methods	ANN	DJF	MAM
TX	Climatol	0.21 (0.17;0.25)	0.16 (0.11;0.22)	0.21 (0.16;0.26)
	HOMER	0.20 (0.12;0.28)	0.13 (0.07;0.19)	0.19 (0.14;0.25)
TN	Climatol	0.24 (0.20;0.28)	0.22 (0.17;0.28)	0.26 (0.21;0.31)
	HOMER	0.29 (0.24;0.34)	0.23 (0.19;0.27)	0.29 (0.23;0.34)
TM	Climatol	0.22 (0.19;0.26)	0.19 (0.13;0.24)	0.24 (0.20;0.28)
	HOMER	0.25 (0.20;0.31)	0.18 (0.13;0.24)	0.24 (0.20;0.27)
DTR	Climatol	-0.04 (-0.07;-0.01)	-0.04 (-0.07;0.00)	-0.04 (-0.08;0.00)
	HOMER	-0.07 (-0.13;0.00)	-0.10 (-0.14;-0.05)	-0.08 (-0.14;-0.01)
RR	Climatol	-2.07 (-3.38;-0.90)	-0.96 (-2.76;0.95)	-2.35 (-5.19;0.32)
	HOMER	-2.34 (-4.00;-1.15)	-1.24 (-3.32;1.00)	-2.56 (-5.54;0.60)
Parameters	Methods	JJA	SON	
TX	Climatol	0.20 (0.16;0.23)	0.27 (0.21;0.33)	
	HOMER	0.18 (0.10;0.26)	0.23 (0.10;0.35)	
TN	Climatol	0.23 (0.19;0.27)	0.26 (0.21;0.30)	
	HOMER	0.28 (0.21;0.33)	0.29 (0.22;0.35)	
TM	Climatol	0.21 (0.18;0.25)	0.26 (0.21;0.31)	
	HOMER	0.23 (0.17;0.30)	0.27 (0.17;0.36)	
DTR	Climatol	0.00 (-0.06;0.00)	0.00 (-0.04;0.05)	
	HOMER	-0.07 (-0.13;-0.01)	-0.11 (-0.20;-0.03)	
RR	Climatol	-3.04 (-8.50;1.68)	-4.52 (-6.61;-1.78)	
	HOMER	-4.05 (-10.17;0.17)	-5.34 (-7.77;-3.00)	

Note: Boldface indicates significant trends at 0.05 level.

Abbreviations: ANN, Annual; DJF, December–January–February; DTR, Diurnal temperature range and RR, Precipitation; JJA, June–July–August; MAM, March–April–May; SON, September–October–November; TM, mean temperature; TN, minimum temperature; TX, maximum temperature.

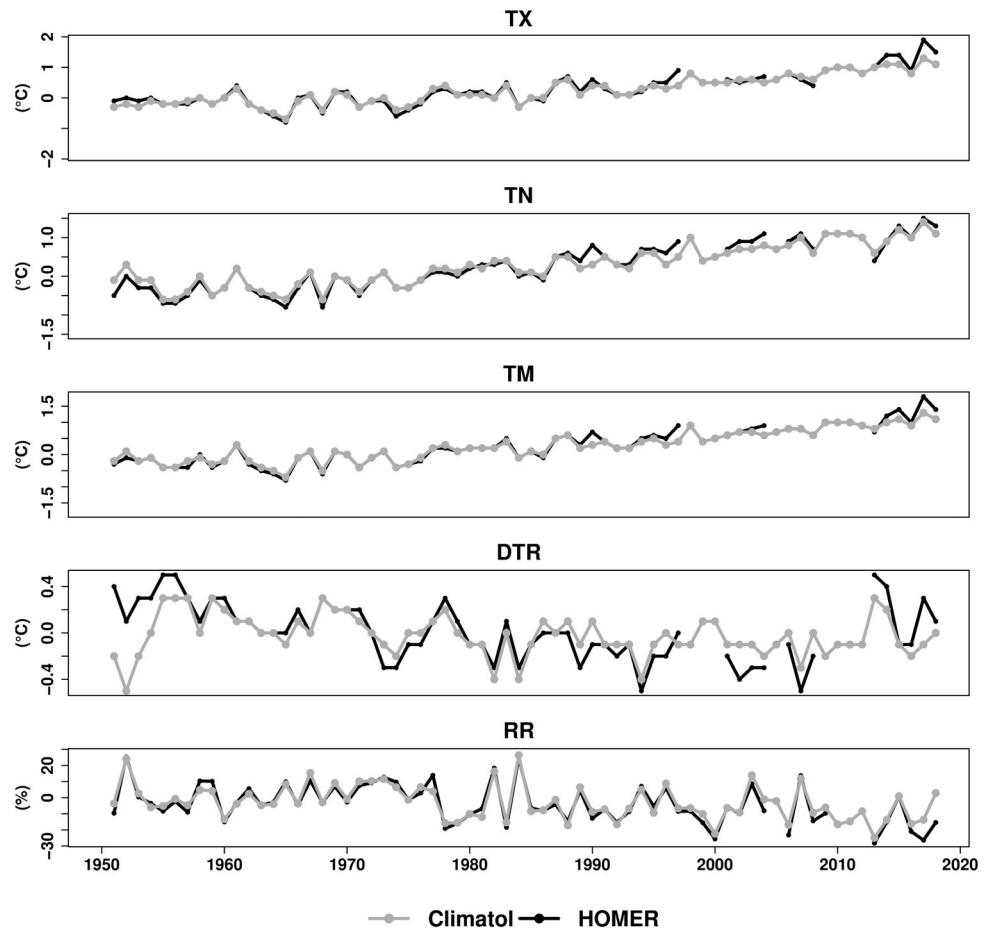
within the framework of the project using a benchmark data set (Guijarro *et al.*, 2019, Guijarro *et al.*, 2018 and Pérez-Zanón *et al.*, 2018).

INQC identifies erroneous (e.g., negative precipitation), suspect (e.g., outliers to the empirical distribution) and collectively suspect (e.g., runs of consecutive values) observations and, based on a flag system, provides information to the analysis for further inspection. The software is flexible and was parameterized to capture the climate of Madagascar by specifying different thresholds for temperatures and precipitation coherent with the study area section. The Extreme Value Approach was used to determine these thresholds. For instance, the highest and lowest temperatures were set at 40 and 0 $^{\circ}\text{C}$, respectively. INQC was applied station-by-station and flagged observations were grouped in Table 3. The application of INQC enabled obvious errors to be identified, such as those in the Fianarantsoa station (Figure 3a), introduced during the digitization and manipulation of the data set, when minimum temperature values were

inadvertently replaced by rainfall values in early January 2018. The software also identified sequences of values that highlighted certain problems in the data set. This happened with the Ivato maximum temperature series, which were provided without the decimal point from 2006 to 2013. These values were compared with the Antananarivo maximum temperature series and SYNOP reports (<http://www.ogimet.com/synops.phtml.en>) for 2006–2013. Unfortunately, most values were validated because of the lack of decision support materials. Another case (Figure 3b) is the series of identical values found at Sainte Marie station in March 2017, combined with interdiurnal values that were too high. These values were errors and could be corrected by using SYNOP reports.

The quality control process also resulted in the validation of extreme values and unusually long spells. For example, a daily value of precipitation exceeding the 500 mm $\cdot\text{day}^{-1}$ pre-set threshold was found on January 21, 1977 (559.1 mm) at the Morondava station. This case

FIGURE 5 Annual regional anomalies of Climatol (grey) and HOMER (black) homogenized data



was caused by Tropical Storm Domitile, which lasted from January 18, to January 23, 1977. Therefore, the value was validated and saved. INQC also detected unusually long spells with no precipitation in Mahajanga (April–November 2014) and Ranohira (April–September 2013). Even though they are statistically suspect, they represent extremely dry seasons and were validated.

The approach adopted for validating flagged values was based on comparing the observations with neighbouring stations and consulting different archives. For the period 1950–1968, values were checked against the archives of the NOAA Central Library (<https://library.noaa.gov/Collections/Digital-Docs/Foreign-Climate-Data/Madagascar-Climate-Data#o39758671>) which stores scans of Malagasy daily climate data from 1935 to 1968. For 1969 to 2018, they were compared with SYNOP reports. Finally, the FIRINGA website (<http://www.firinga.com/activite-cyclonique/ocean-indien.html>), which archives tropical cyclone seasons in the South-West Indian Ocean Basin, was used for rainfall events associated with tropical cyclone seasons from 1969/1970 to 2018/2019. However, we were aware that precautions should be taken with synoptic messages as they might offset the absolute values of indices. Trends could be

stable, as shown by the comparison of SYNOP and ECA&D data for temperature and precipitation (Besselaar *et al.*, 2012). Moreover, the FIRINGA website highlighted the events without giving any observational values on precipitation, although it helped to make a decision between replacing the value by missing data or keeping the current value. Table 3 summarizes the QC process. A total of 1,182 values were checked, from which 50 were validated, 401 were corrected and 731 set to missing.

3.1.2 | Data homogenization

Non-climatic factors such as station relocations, changes in instruments, observation procedures and local environment can affect the homogeneity of long-term observational. Inhomogeneities could cause sudden and gradual biases in climate data and impact on climate analysis, specifically on climate trends (Peterson *et al.*, 1998; Trewin, 2010). Thus, homogenization, or at least homogeneity assessment, is a mandatory preliminary step before tackling any sound climatological analysis. From the large number of different homogenization

TABLE 5 Selected CLIMIND climate indices and its ETCCDI equivalent

Elements	ClimInd	Description	ETCCDI	Unit
Temperature	CDD	Cold spell duration	CSDI*	Days
	WSD	Warm spell duration	WSDI*	Days
	CN	Percentage of days when TN < 10th percentile	TN10P	%
	CD	Percentage of days when TX < 10th percentile	TX10P	%
	GTN	Mean of TN	TNMean	°C
	GTX	Mean of TX	TXMean	°C
	NTN	Minimum of TN	TNn	°C
	NTX	Minimum of TX	TXn	°C
	XTN	Maximum of TN	TNx	°C
	XTX	Maximum of TX	TXx	°C
	TN	Tropical nights with TN > 20°C	TR20	Days
	D32	Days with TX > 32°C	-	Days
	CSD	Maximum consecutive summer days (MCSU25)	-	Days
	SUD	Summer days with TX > 25°C	SU25	Days
	VCD	Days when TN < 1st percentile (TN1P)	-	Days
	VWD	Days when TX > 99th percentile (TX99P)	-	Days
	WN	Percentage of days when TN > 90th percentile	TN90P	%
	WD	Percentage of days when TX > 90th percentile	TX90P	%
	DTR	Mean difference between TX and TN	DTR	°C
	ETR	Difference between the maximum TX and the minimum TN	-	°C
	VDTR	Mean absolute day-to-day difference in DTR	-	°C
Precipitation	D50mm	Heavy precipitation days with RR > 50 mm	RR50mm*	Days
	D95P	Very wet days with RR > 95p	-	Days
	DD	Dry days with RR < 1 mm	-	Days
	DR1mm	Wet days with RR ≥ 1 mm	RR1mm*	Days
	LDP	Maximum length of consecutive dry days (RR < 1 mm)	CDD	Days
	LWP	Maximum length of consecutive wet days (RR ≥ 1 mm)	CWD	Days
	R10mm	Days precipitation ≥ 10 mm	RR10mm	Days
	R20mm	Days precipitation ≥ 20 mm	RR20mm	Days
	R95TOT	Precipitation exceeding 95p divided by total precipitation	R95P*	%
	R99TOT	Precipitation exceeding 99p divided by total precipitation	R99P*	%
	SDII	Precipitation in wet days divided by number of wet days	SDII	mm·days ⁻¹
	RTI	Total precipitation	PRCPTOT	mm
	RTWD	Total precipitation in wet days (PRCWTOT)	-	mm
	RX	Highest amount of daily precipitation	RX1day	mm
	RX5D	Maximum consecutive 5-day precipitation	RX5day	mm
	SPEI	Standardized precipitation-evapotranspiration index calculated at 3- and 12-month timescale	-	z-units

Note: Dash (-) means climate indices are not included in ETCCDI. Asterisk (*) indicates that climate indices were not calculated in Vincent et al (2011). Abbreviations: RR daily rainfall; TX, daily maximum temperature; TN, daily minimum temperature.

approaches, we selected Climatol (see Guijarro, 2018) and used the source code of the development version (see <http://www.climatol.eu/>), extensively tested via benchmarking in the MULTITEST and INDECIS projects. We chose to detect inhomogeneities over monthly data and then adjust to the daily scale instead of direct detection from daily values. This improved the signal to noise ratio and the performance of the method (Guijarro, 2018). Climatol detects breakpoints (potential inhomogeneities) using a modified version of SNHT (see Alexandersson, 1986; Alexandersson and Moberg, 1997;

Moberg and Alexandersson, 1997). The monthly adjustments are calculated by orthogonal regression or Reduced Major Axis in which all scatter points are adjusted to a regression line by minimizing the perpendicular distance.

The data set was also homogenized with HOMER for comparison purposes. HOMER is the result of the European COST Action ES0601(2006–2011) (Venema *et al.*, 2012) and uses completely different detection and adjustment methods (see Mestre *et al.*, 2013). As HOMER only adjusts annual and monthly climate data (Mestre

TABLE 6 Regional trends with the confidence intervals (in brackets)

Index (Climind/ Rclimdex)	Trends (confidence interval)	Unit/ decade
CDD/CSDI	-2.28 (-3.20; -1.48)	Days
WSD/WSDI	3.81 (1.98; 6.01)	Days
CN/TN10P	-1.52 (-1.90; -1.18)	%
CD/TX10P	-1.31 (-1.72; -0.86)	%
GTN/TNMean	0.24 (0.20; 0.28)	°C
GTX/TXMean	0.21 (0.17; 0.25)	°C
NTN/TNn	0.29 (0.19; 0.39)	°C
NTX/TXn	0.11 (0.00; 0.22)	°C
XTN/TNx	0.24 (0.11; 0.36)	°C
XTX/TXx	0.23 (0.07; 0.36)	°C
TN/TR20	7.72 (6.29; 9.22)	Days
D32	0.43 (0.18; 0.66)	Days
CSD/MCSU25	4.41 (1.76; 6.90)	Days
SUD/SU25	5.40 (4.39; 6.48)	Days
VCD/TN1P	-0.79 (-1.12; -0.49)	Days
VWD/TX99P	0.82 (0.17; 1.54)	Days
WN/TN90P	3.01 (1.84; 4.28)	%
WD/TX90P	2.38 (1.27; 3.49)	%
DTR/DTR	-0.04 (-0.07; -0.01)	°C
ETR	-0.05 (-0.26; 0.15)	°C
VDTR	0.01 (-0.03; 0.04)	°C

Note: Boldface indicates significant at 0.05 level.

et al., 2013), it was complemented by the approach described in Vincent *et al.* (2002) for temperature. For precipitation, annual factors were directly applied to the daily data. HOMER needs a limited amount of data, so the data set was reduced to 19 stations.

HOMER was run in a semi-automatic mode (i.e., assessing whether to accept or reject the breakpoints suggested by the test; metadata was used to validate breakpoints) meanwhile Climatol was run in a fully automatic mode. Despite the fact that a larger number of breakpoints were detected in HOMER (see Figure 4 for illustration), the regional trends were fairly similar, as suggested by Table 4 and Figure 5, which shows regional time series. Both homogenized data sets, produced independently and using completely different approaches, suggest a strong warming across the island, uniformly distributed throughout the year and slightly higher for night-time temperatures, which results in a small reduction in the DTR. These warming trends were coupled with uniform drying trends.

Once we remarked that both approaches return similar results, we used the data set homogenized with

Climatol, since it includes a larger number of stations and the fact that it can be run safely in fully automated mode, which will enable our analysis to be seamlessly updated when additional data records become available. In addition, Climatol uses an iterative process to fill gaps in mean and standard deviation calculation, a task not performed by HOMER (Figure 5).

3.2 | Methods

3.2.1 | Climate indices calculation

Annual and seasonal climate indices were obtained using the quality-controlled and homogenized data set described in the previous sections. They were calculated using the CLIMIND package, developed by the INDECIS project (see Domínguez-Castro *et al.*, 2020), which includes 125 sector-oriented indicators computed from surface air temperature, precipitation, relative humidity, wind speed, cloudiness, solar radiation and snow cover. Due to the characteristics of our data set, we calculated a subset of 37 climate indices which rely solely on temperature or/and precipitation. The Standardized Precipitation Evapotranspiration Index (SPEI, Vicente-Serrano *et al.*, 2010) factors in the climatic water balance, determined from the difference between precipitation and reference evapotranspiration (ET0). Hargreaves formula (Hargreaves, 1994) was used to calculate ET0 because there was not sufficient data available to apply more robust procedures (e.g., the Penman-Monteith, which needs data on wind speed, solar radiation and relative humidity). CLIMIND expands the set of ETCCDI indicators that were used in a previous paper by Vincent *et al.* (2011) covering the Western Indian Ocean countries. Table 5 shows the set of 37 climate indices used, and a brief description of the indicator (see Domínguez-Castro *et al.*, 2020 for a full description). For the sake of comparison with Vincent *et al.* (2011) and with other regional or global papers, we added a column with the ETCCDI names.

3.2.2 | Area averaging and trend calculation

To extract regional time series, we adopted the approach by Vincent *et al.* (2011) and calculated the average departures to the WMO reference 1961–1990 period for temperature and precipitation. However, the departures were divided by the 1961–1990 mean for total precipitation (RTI or PRCPTOT), total precipitation wet days (RTWD), maximum precipitation (RX or RX1day) and maximum 5-day precipitation (RX5D or RX5day). Thereafter,

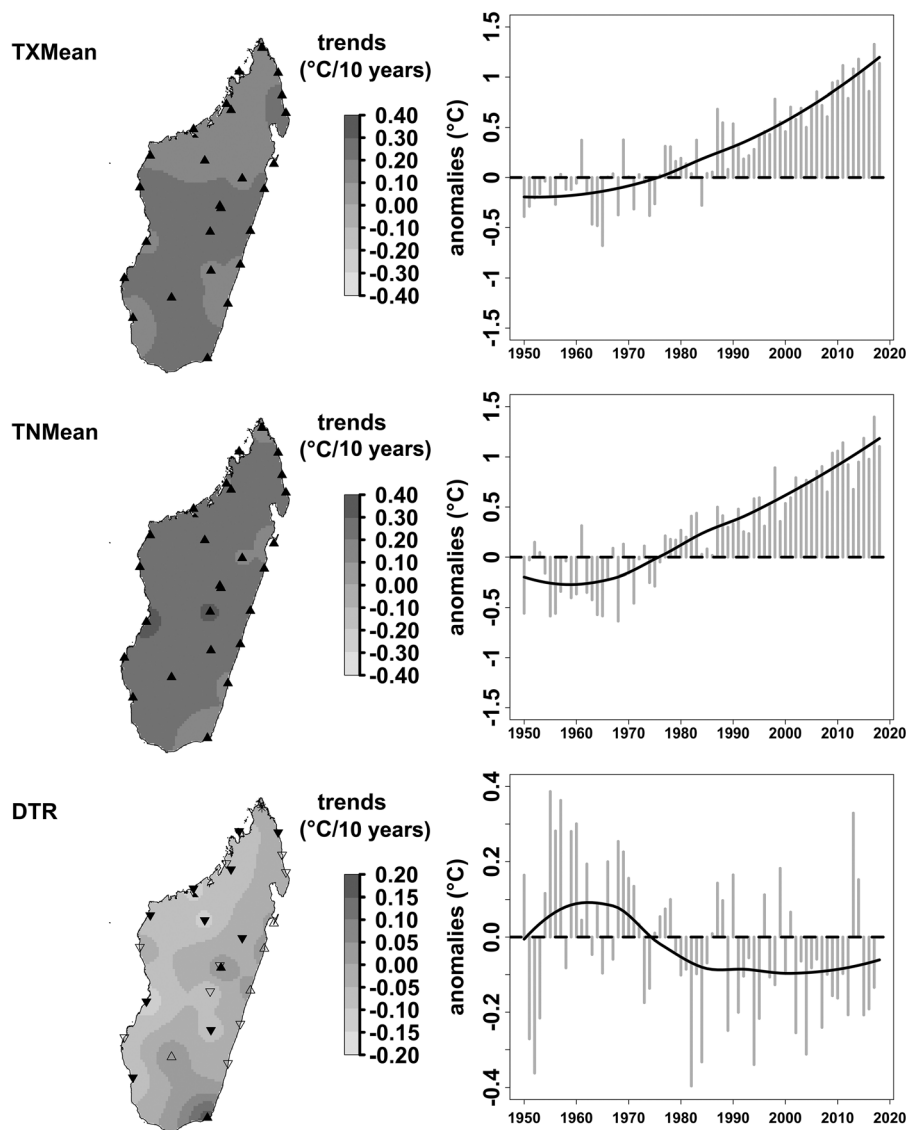


FIGURE 6 Station-by-station decadal trends and annual regional anomalies (fitted curve calculated using a LOESS function) of TXMean, TNMean and DTR. Solid point-up and point-down triangles indicate significant positive and negative trends at 0.05 level. Asterisk means no trend. Shaded colours are interpolation from the inverse distance weighted (IDW) function

regional time series were obtained by averaging all stations.

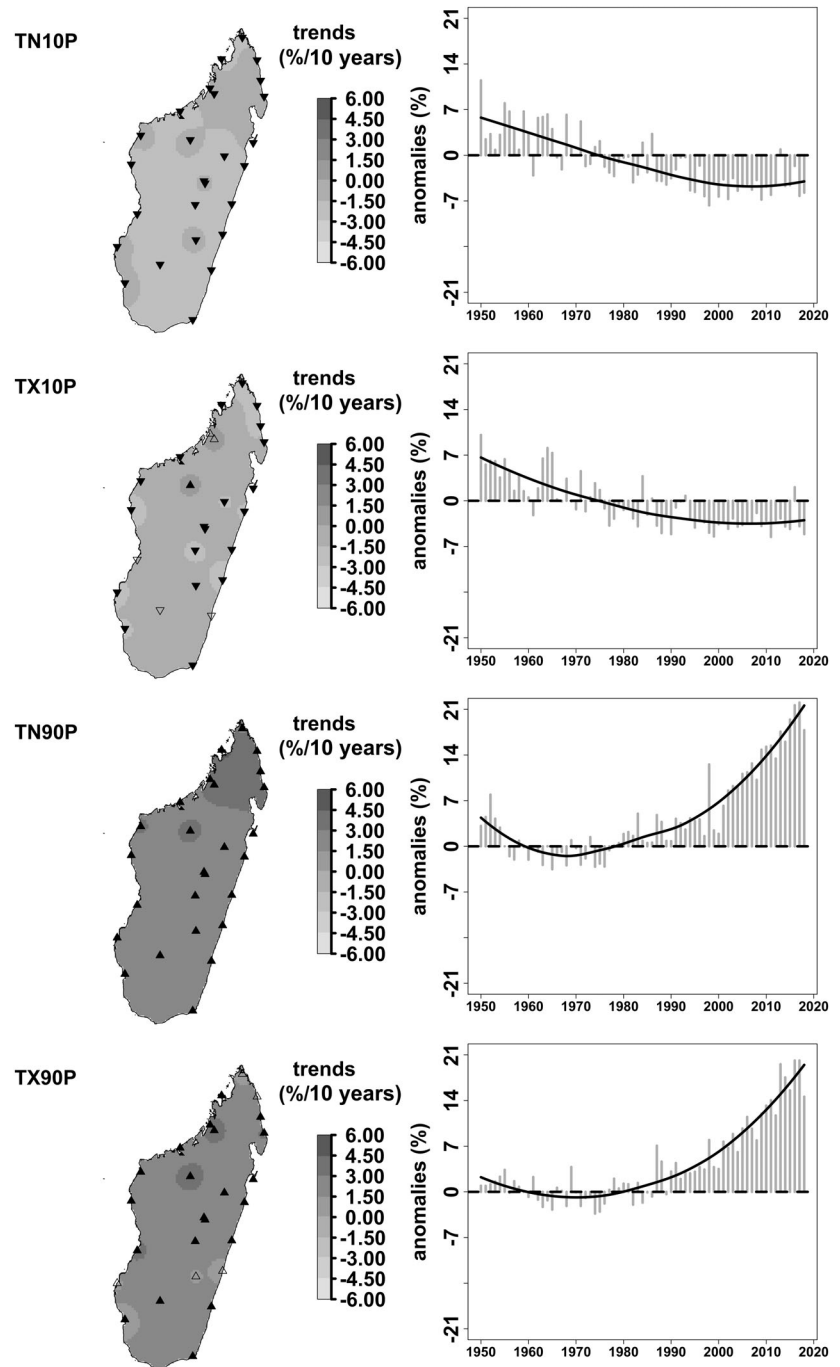
We calculated the drought characteristics (i.e., intensity, magnitude and duration) based on 3- and 12-month SPEI series. Drought events occur if 3- and 12-month SPEI values are lower than zero, similar to Domínguez-Castro *et al.* (2019). Drought duration is the period of consecutive years with SPEI < 0. Drought magnitude and maximum intensity correspond to the sum and maximum severity of absolute values in drought duration, respectively. We adopted the z-score transformation as it is commonly used for drought monitoring (e.g., Morid *et al.*, 2006; Abrha and Hagos, 2019; Byrd *et al.*, 2020). Therefore, drought characteristics were transformed to z-score using the Equation (1) before calculating trends:

$$Z_i = \frac{X_i - \bar{X}}{\sigma} \quad (1)$$

Where i is the year from 1950 to 2018; Z_i is the z-score at year i ; X_i is the drought characteristic at year i ; \bar{X} is the mean of the drought characteristic; σ is the standard deviation of the drought characteristic.

Trends and their significance at 0.05 level are calculated for each index, station and regional time series on an annual scale, using the Sen slope method (Sen, 1968) as implemented by Zhang (Zhang *et al.*, 2000). Calculations were made with the 'zyp' R package (Bronaugh and Werner, 2019). This package implements the method and was used in many papers, such as Barry *et al.* (2018) and Yosef *et al.* (Yosef *et al.*, 2019; Yosef *et al.*, 2021). The lower and upper limits of trend confidence interval are at 0.025 and 0.975, respectively. Both approaches—area averaging and trend calculation—have been used in similar papers (e.g., Aguilar *et al.*, 2005; Aguilar *et al.*, 2009; Vincent *et al.*, 2011; Barry *et al.*, 2018).

FIGURE 7 Station-by-station decadal trends and annual regional anomalies (fitted curve calculated using a LOESS function) of TN10P, TX10P, TN90P and TX90P. Solid point-up and point-down triangles indicate significant positive and negative trends at 0.05 level. Shaded colours are interpolation from the inverse distance weighted (IDW) function



4 | RESULTS

4.1 | Temperature indices

Regional temperature indices present a temporal evolution in agreement with warming (Table 6 and Figures 6 and 7). All trends are significant at the 0.05 level, except for ETR and VDTR, which both show the evolution of differences within daytime and night-time temperature and suggest a significant general decrease of $-0.04^{\circ}\text{C}/\text{decade}$, as confirmed by the DTR. Also, trends in night-

time indices, that is, those computed over minimum temperatures, are higher than for daytime (maximum temperature) indices. For example, warm nights indicate increasing trend of $3.01\%/decade$, whereas warm days show a positive trend of $2.38\%/decade$. We observe the same pattern when comparing the decrease in cold nights ($-1.52\%/decade$) versus the decrease in cold days ($-1.32\%/decade$). These four indices illustrate another feature of warming in Madagascar: it is due to both the occurrence of warmer weather and the suppression of cold weather, but the former mostly dominates. These

TABLE 7 Percentage of stations with positive significant, positive non-significant, negative significant and negative non-significant trends

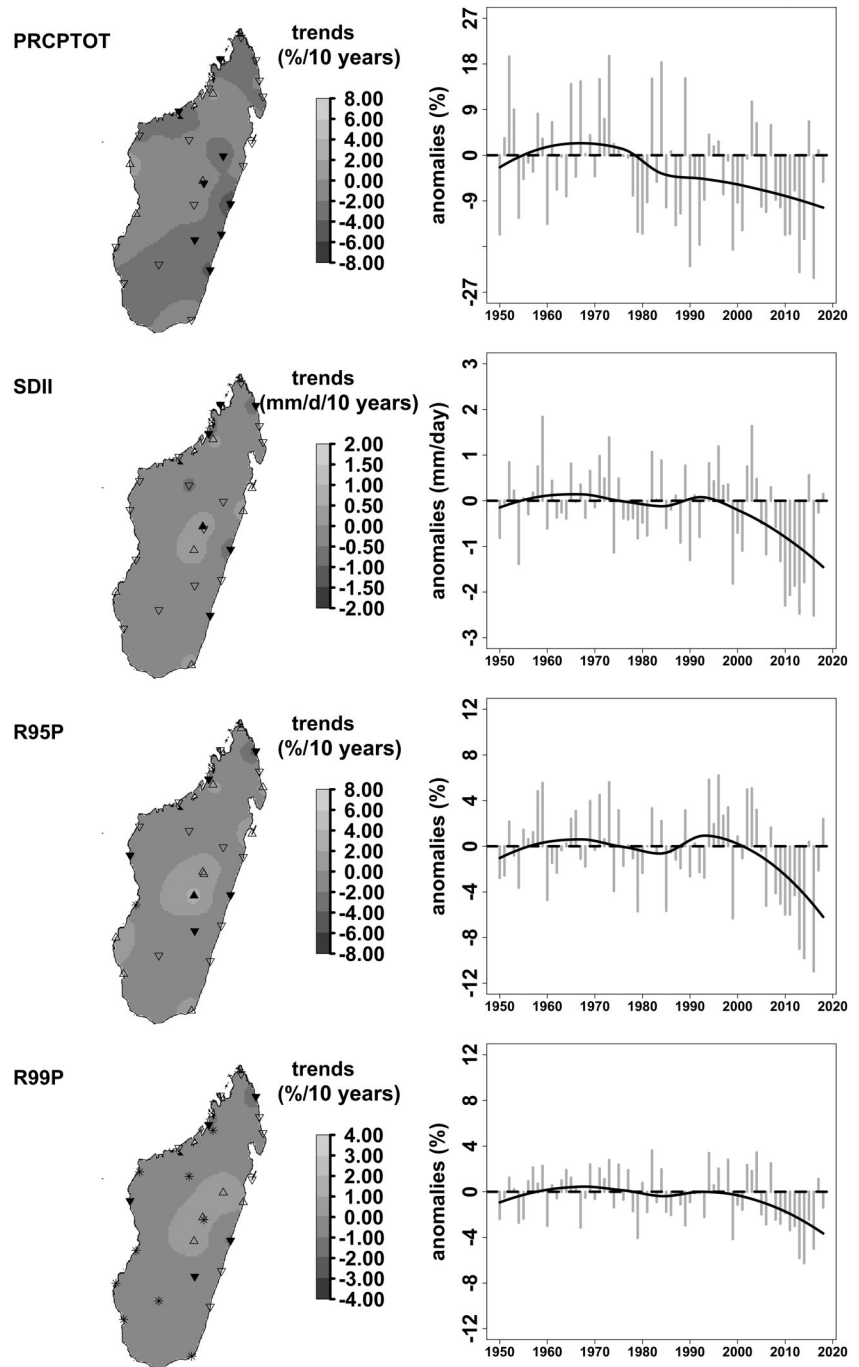
Index (Climind/Rclimdex)	Positive trends (%)		Negative trends (%)	
	Significant	Non-significant	Significant	Non-significant
CDD/CSDI	0	0	66.7	14.8
WSD/WSDI	59.3	11.1	0	0
CN/TN10P	0	0	100	0
CD/TX10P	3.7	7.4	77.8	11.1
GTN/TNMean	100	0	0	0
GTX/TXMean	100	0	0	0
NTN/TNn	66.7	29.6	0	3.7
NTX/TXn	44.4	37	18.5	0
XTN/TNx	70.4	29.6	0	0
XTX/TXx	51.9	37	0	7.4
TN/TR20	88.9	0	0	0
D32	14.8	7.4	0	7.4
CSD/MCSU25	63	7.4	3.7	0
SUD/SU25	55.6	14.8	0	0
VCD/TN1P	0	0	55.6	37
VWD/TX99P	33.3	18.5	0	3.7
WN/TN90P	100	0	0	0
WD/TX90P	77.8	22.2	0	0
DTR	7.4	14.8	37	37
ETR	11.1	44.4	22.2	22.2
VDTR	11.1	37	14.8	22.2

Index (Climind/Rclimdex)	Trends (confidence interval)		Unit/decade
	1950–2018	2000–2018	
D50MM/RR50mm	-0.20 (-0.32; -0.07)	-0.11 (-0.29; 0.07)	Days
D95P	-0.54 (-0.88; -0.25)	-0.21 (-0.56; 0.06)	Days
DD	0.59 (-0.29; 1.49)	-0.36 (-0.88; 0.29)	Days
DR1mm/RR1mm	-0.60 (-1.45; 0.26)	0.30 (-0.29; 0.79)	Days
LDP/CDD	1.09 (-0.46; 2.71)	-0.41 (-1.18; 0.25)	Days
LWP/CWD	0.02 (-0.12; 0.16)	-0.04 (-0.16; 0.04)	Days
R10mm/RR10mm	-0.87 (-1.35; -0.39)	-0.08 (-0.58; 0.33)	Days
R20mm/RR20mm	-0.67 (-1.01; -0.35)	-0.25 (-0.65; 0.25)	Days
R95TOT/R95P	-0.51(-1.07;0.14)	-0.65 (-1.05; -0.11)	%
R99TOT/R90P	-0.39 (-0.71; -0.07)	-0.24 (-0.58; 0.01)	%
SDII	-0.18 (-0.31; -0.02)	-0.12 (-0.30; 0.06)	mm·days ⁻¹
RTI/PRCPTOT	-2.07 (-3.38; -0.90)	-0.51 (-1.61; 0.46)	%
RTWD/PRCWTOT	-2.10 (-3.35; -0.91)	-0.51 (-1.63; 0.41)	%
RX/RX1day	-1.52 (-2.85; -0.19)	-1.24 (-2.16; 0.13)	%
RX5D/RX5day	-1.85 (-3.43; -0.29)	-1.10 (-2.76; 0.04)	%

TABLE 8 Regional trends with the confidence intervals (in brackets)

Note: Boldface indicates significant at 0.05 level.

FIGURE 8 Station-by-station decadal trends and annual regional anomalies (fitted curve calculated using a LOESS function) of PRCPTOT, SDII, R95P and R99P. Solid point-up and point-down triangles indicate significant positive and negative trends at 0.05 level. Asterisk means no trend. Shaded colours are interpolation from the inverse distance weighted (IDW) function



two features are also evident from other indices, for example, the annual average of daily minimum temperatures (GTN) and the annual mean of daily maximum temperature (GTX). The seasonal analysis shows that warming occurs across the four seasons and is strongest in spring (Table 4). Finally, looking at trends at station level, even though noticeable differences in values are evident from Figures 6 and 7, they do not present a clear spatial pattern and uniform warming across the island. Table 7 shows the percentage of stations with significant positive/negative trends for each index.

4.2 | Precipitation indices

The analysis of the regional time series of precipitation indices and their trends in Madagascar displays an evolution towards drier conditions. The first five decades of the study period show values fluctuating around the long-term mean. At the turn of the century, precipitation decreases, and we observe the same pattern for the different climate indices. Not only PRCPTOT decays ($-2.07 \text{ mm-decade}^{-1}$, significant at the 0.05 level), but also the number of rainfall

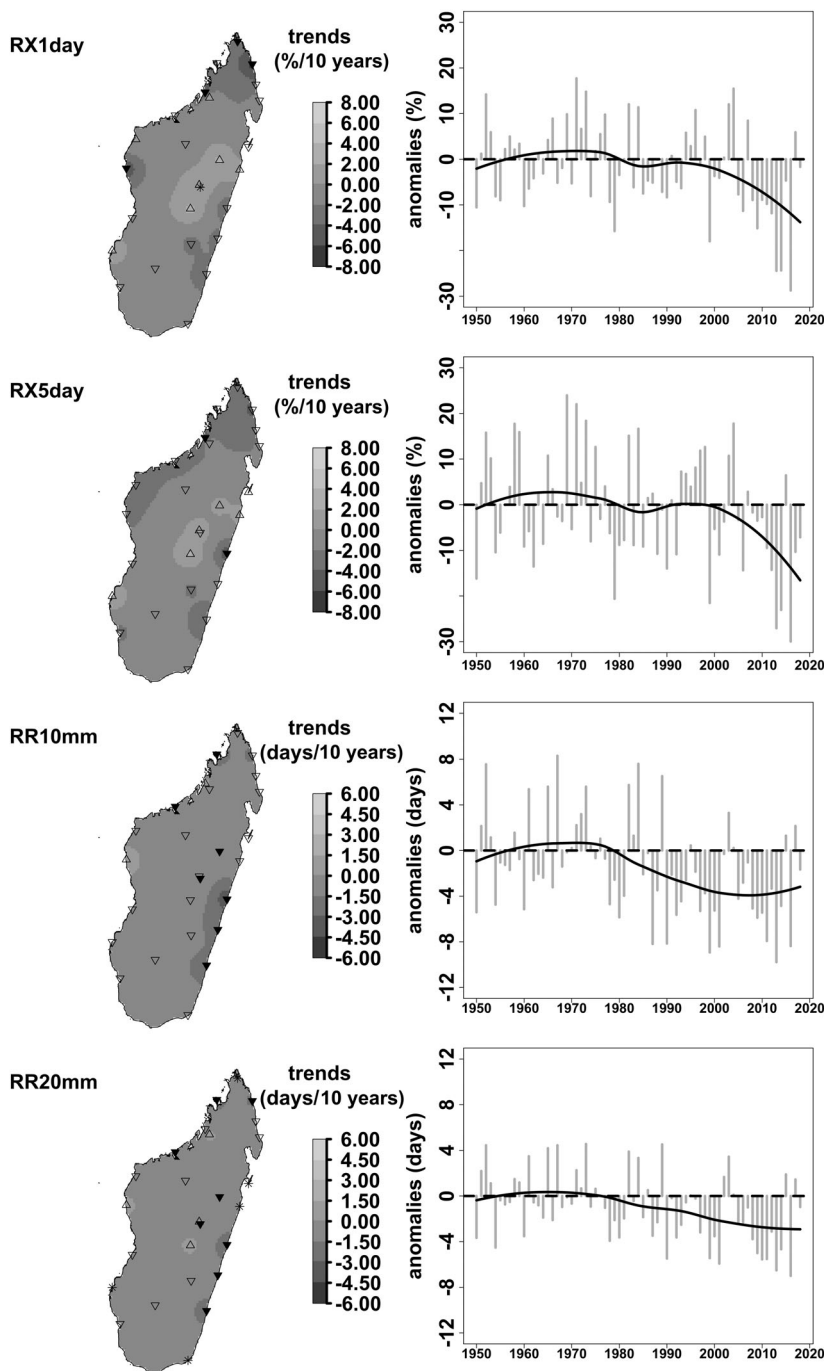


FIGURE 9 Station-by-station decadal trends and annual regional anomalies (fitted curve calculated using a LOESS function) of Rx1day, Rx5day, RR10 mm and RR20 mm. Solid point-up and point-down triangles indicate significant positive and negative trends at 0.05 level. Asterisk means no trend. Shaded colours are interpolation from the inverse distance weighted (IDW) function

days per year falls ($-0.60 \text{ days}\cdot\text{decade}^{-1}$) in the same proportion as dry days raise ($0.59 \text{ days}\cdot\text{decade}^{-1}$). The indices based on the upper tail of the distribution also display negative trends (e.g., the heavy precipitation fraction, R95TOT, $-0.51 \text{ mm}\cdot\text{decade}^{-1}$; SDII, $-0.18 \text{ mm}\cdot\text{decade}^{-1}$). The longest dry period (LDP) displays increasing trend of $1.09 \text{ days}\cdot\text{decade}^{-1}$. These trends suggest a shift in the magnitude of precipitation, driven by fewer precipitation events leading towards smaller accumulations. Table 8 shows the trends for

the 1950–2018, also trends for the 2000–2018 period of intensified drying.

As expected, observed trends in precipitation indices show more spatial diversity than those observed in temperature indices. Most significant drying trends occur in the east coast area (Figures 8 and 9). Moreover, we remark a large percentage of stations with negative trends (mostly non-significant) for all indices except for dry days (DD) and the longest dry period (LDP) for the 2000–2018 period of intensified drying (Table 9).

TABLE 9 Percentage of stations with positive significant, positive non-significant, negative significant and negative non-significant trends

Index (Climind/Rclimdex)	Positive trends (%)				Negative trends (%)			
	Significant		Non-significant		Significant		Non-significant	
	1950–2018	2000–2018	1950–2018	2000–2018	1950–2018	2000–2018	1950–2018	2000–2018
D50mm/RR50mm	3.7	0.0	11.1	29.8	25.9	7.4	29.6	40.7
D95P	0.0	3.7	14.8	14.8	37.0	11.1	37.0	55.6
DD	25.9	14.8	55.6	33.3	7.4	14.8	11.1	22.2
DR1mm/RR1mm	7.4	14.8	11.1	22.2	29.6	11.1	51.9	40.7
LDP/CDD	25.9	0.0	40.7	44.4	3.7	11.1	25.9	37.0
LWP/CWD	7.4	7.4	14.8	22.2	7.4	11.1	33.3	44.4
R10mm/RR10mm	0.0	3.7	11.1	25.9	25.9	3.7	63.0	51.9
R20mm/RR20mm	0.0	0.0	14.8	18.5	29.6	3.7	37.0	63.0
R95TOT/R95P	3.7	3.7	33.3	29.6	22.2	11.1	37.0	55.6
R99TOT/R90P	0.0	0.0	14.8	18.5	18.5	3.7	33.3	37.0
SDII	3.7	0.0	22.2	37.0	18.5	7.4	55.6	55.6
RTI/PRCPTOT	0.0	0.0	14.8	29.6	29.6	7.4	55.6	63.0
RTWD/PRCWTOT	0.0	0.0	11.1	25.9	29.6	7.4	59.3	63.0
RX/Rx1day	0.0	0.0	25.9	22.2	18.5	11.1	51.9	66.7
RX5D/Rx5day	0.0	3.7	22.2	18.5	7.4	7.4	70.4	70.4

4.3 | Drought indices

Figure 10 shows the regional drought events (black bars) from 1950 to 2018. Maximum and minimum drought events (49 and 34) appear at the beginning (September–October–November) and end (March–April–May) of the wet season, respectively, a situation that makes difficult to establish a cultural calendar in Madagascar. More severe drought events occur after the 1980s, which are more consecutive during the 2000–2018 period of intensified drying detected in the precipitation section (see Section 4.2). Figure 11 and Figure 12 present station-by-station decadal trends of drought magnitude and duration respectively. They point to drought being a local phenomenon in Madagascar. For instance, south-eastern stations (e.g., Farafangana and Ranohira) indicate large increasing trends in the magnitude and duration of drought annually. More than 70% of stations record positive non-significant drought characteristic trends at 0.05 level at annual and seasonal scales (except for December–January–February). Table 10 shows the percentage of stations with positive significant, positive non-significant, negative significant and negative non-significant trends at annual and seasonal scales.

5 | DISCUSSION

This paper generated very robust daily records by adopting the latest methods and tools on daily data quality control (QC) and homogenization. These steps were essential for a robust assessment of climate trends. According to Hunziker *et al.* (2017), QC procedures might improve a part of the data homogeneity specifically for the sparse network. We scrupulously checked 1,182 values detected as errors by INQC developed within the framework of the INDECIS project. Homogenization was a crucial step in climate analysis, as pointed out by Squintu *et al.* (2020). We performed daily homogenization with Climatol and HOMER, complemented by the approach described in Vincent *et al.* (2002). They were in good agreement as far as timing of breakpoints were concerned and showed a good overlap of annual regional anomalies. Moreover, annual and seasonal regional trends were almost consistent and significant at the 0.05 level. Climatol homogenization improved the accuracy and reliability of indices' trends, as Skrynyk *et al.* (2021) concluded. Therefore, climate indices were calculated using the daily homogenized series with Climatol.

This paper attempted use climate indices to increase knowledge on how climate changed in Madagascar from 1950 to 2018. As expected, due to the nature of both

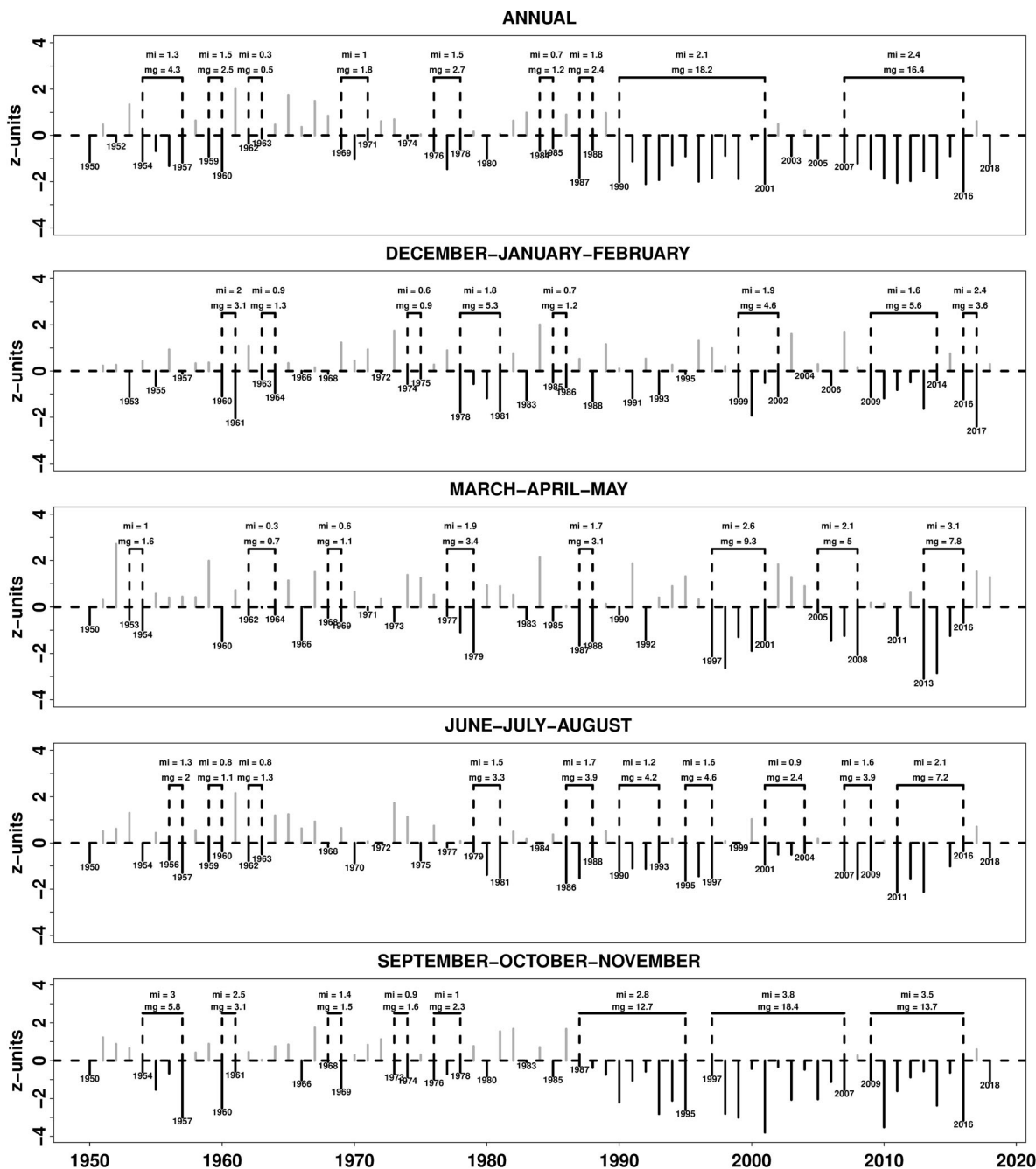
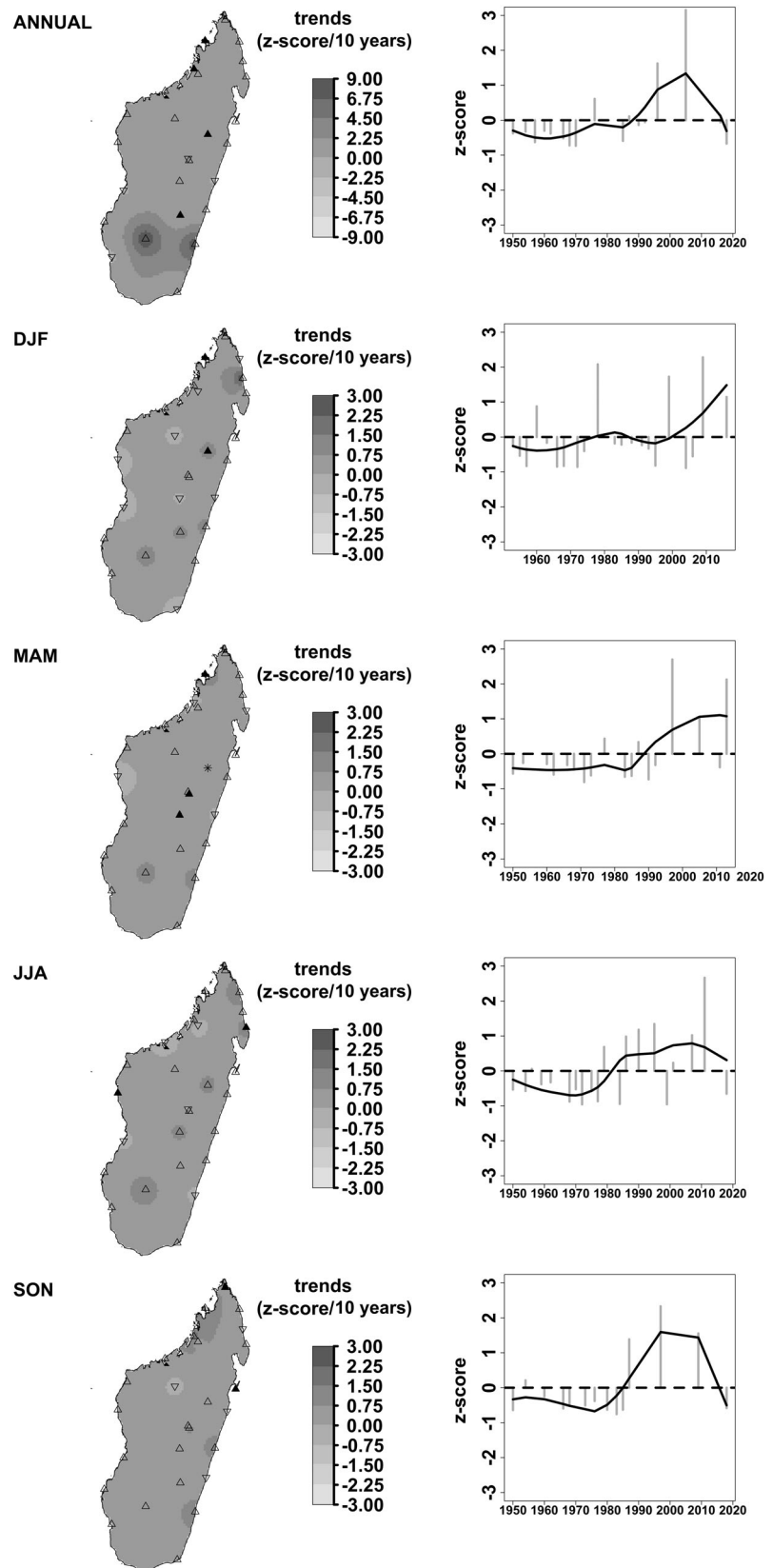


FIGURE 10 Regional drought characteristics from 3- and 12-month SPEI series. 'mi' and 'mg' indicate maximum intensity and magnitude values during consecutive drought periods (black bars), respectively

meteorological elements (i.e., temperature and precipitation), our analysis demonstrated that the changes in temperature had a higher degree of spatial coherence than in precipitation. Moreover, changes in both were noticeable, as suggested by the regional and station-by-station trends, most of which were significant at the 0.05 level for all indices during the last seven decades. Changes in temperature corroborated with warming. Changes in precipitation were moving towards drier conditions. Changes in drought characteristics indicated more consecutive drought events.

In agreement with Tadross *et al.* (2008), we found that warming occurred across all seasons and the highest warming appeared in spring. The web portal on climate change in the Southwest Indian Ocean (<http://regionalclimate-change.sc/>) provides a climate profile for member countries and we found that annual mean temperature increased in the region. However, our regional average of annual mean temperature was 0.02 and 0.08°C·decade⁻¹ higher than for Comoros and Seychelles, respectively. Tara James *et al.* (Tara James and

FIGURE 11 Station-by-station decadal trends and annual regional anomalies (fitted curve calculated using a LOESS function) of drought magnitude. Solid point-up and point-down triangles indicate significant positive and negative trends at 0.05 level. Asterisk means no trend. Shaded colours are interpolation from the inverse distance weighted (IDW) function. DJF, December–January–February; MAM, March–April–May; JJA, June–July–August; SON, September–October–November



Stacia, 2014) wrote that mean annual temperature had increased $0.15^{\circ}\text{C}\cdot\text{decade}^{-1}$ in Mauritius, which was $0.07^{\circ}\text{C}\cdot\text{decade}^{-1}$ lower than our trend. Our regional mean

of annual maximum temperature trend was about 0.02 and $0.05^{\circ}\text{C}\cdot\text{decade}^{-1}$ higher than in Vincent *et al.* (2011) and Barry *et al.* (2018). The regional mean of annual

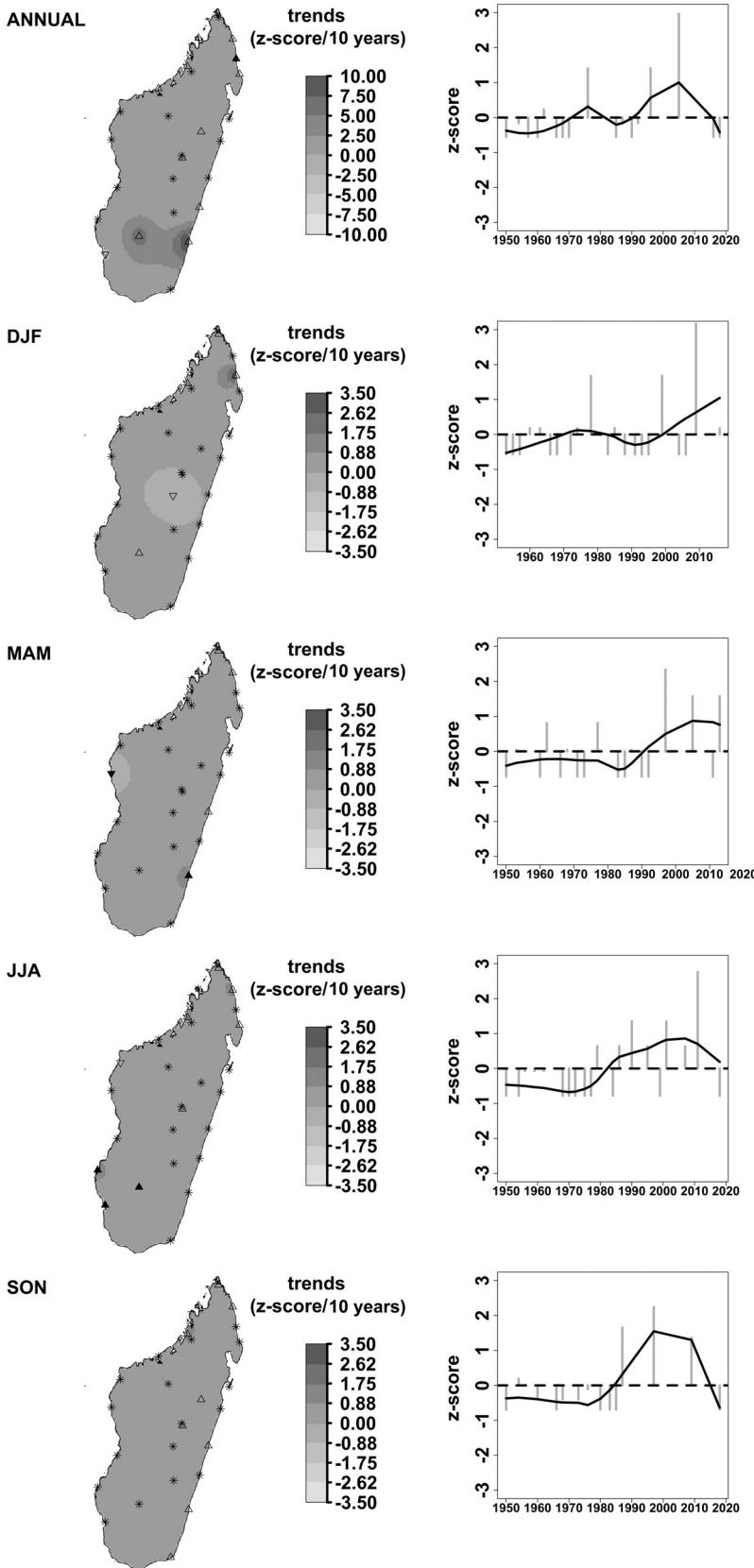


FIGURE 12 Station-by-station decadal trends and annual regional anomalies (fitted curve calculated using a LOESS function) of drought duration. Solid point-up and point-down triangles indicate significant positive and negative trends at 0.05 level. Asterisk means no trend. Shaded colours are interpolation from the inverse distance weighted (IDW) function. DJF, December–January–February; MAM, March–April–May; JJA, June–July–August; SON, September–October–November

minimum temperature was also about $0.04^{\circ}\text{C}\cdot\text{decade}^{-1}$ smaller than in Barry *et al.* (2018). The weakest and strongest regional trends were observed in summer (DJF)

and spring (SON) for mean temperature. The opposite was observed in South Africa according to Kruger and Nxumalo (2017)). As also pointed out by Alexander

TABLE 10 Percentage of stations with positive significant, positive non-significant, negative significant and negative non-significant trends at the annual and seasonal scales

Index	Timescale	Positive trends (%)		Negative trends (%)	
		Significant	Non-significant	Significant	Non-significant
Magnitude	ANNUAL	14.8	70.4	0	14.8
	DJF	11.1	59.3	0	29.6
	MAM	11.1	70.4	0	14.8
	JJA	7.4	74.1	0	18.5
	SON	7.4	74.1	0	18.5
Duration	ANNUAL	7.4	37	0	3.7
	DJF	3.7	18.5	0	3.7
	MAM	7.4	14.8	3.7	0
	JJA	11.1	18.5	0	3.7
	SON	0	33.3	0	0

et al. (2006), Xu *et al.* (2013) and Barry *et al.* (2018), we observed a significant decrease in regional trends of the diurnal temperature range (DTR). This change was observed in 37% of our stations versus 49% of Chinese stations by Xu *et al.* (2013). Vincent *et al.* (2011), using a shorter and less complete version of the Malagasy climate data presented here, also pointed out the negative trend in DTR, although it was non-significant. Our findings also aligned with Niang *et al.* (2015), presented for the whole of Africa, including Madagascar. We noticed that extreme temperature indices were highly significant at 0.05 level, but those for the daily minimum temperature were most meaningful, similar to those in Israel indicated by Yosef *et al.* (2019). As pointed out by Aguilar *et al.* (2005), Alexander *et al.* (2006), New *et al.* (2006), Aguilar *et al.* (2009), Vincent *et al.* (2011), Xu *et al.* (2013), Whan *et al.* (2014), Abatan *et al.* (2016), Kruger and Nxumalo (2017), Barry *et al.* (2018) and Dunn *et al.* (2020), we observed a significant increase in warm nights and days, and a decrease in cold ones. The majority of stations (100% for night-time indices and 77.8% for daytime indices) indicated these warming trends, although Xu *et al.* (2013) observed a lower percentage for China. In addition, changes were more noticeable for high extremes (TX90P and TN90P) than low extremes (TX10P and TN10P) and their regional trend values were smaller and larger respectively compared with Vincent *et al.* (2011). Moreover, very high extremes (TX99P) and very low extremes (TN1P) had significant positive trends (observed in 33.3% of stations) and significant negative trends (observed in 55.6% of stations) respectively. Finally, our tropical nights (TR20) and summer days (SU25) regional trend values were also about 2.58 and 0.68 day-decade⁻¹ higher than in Vincent *et al.* (2011).

Precipitation changes were less significant and non-coherent spatially than in temperature, as highlighted by New *et al.* (2006), Tadross *et al.* (2008), Vincent

et al. (2011), Barry *et al.* (2018), Yosef *et al.* (2019) and Dunn *et al.* (2020). However, a significant decreasing regional trends was mostly explored for all indices except for dry days (DD), longest dry period (LDP) and the longest wet period (LWP). The reduction in total precipitation (PRCPTOT) was then associated with the reduction in heavy precipitation indices (e.g., RR50mm, RR20mm, RR10mm, R95TOT and R99TOT), the intensity of precipitation (SDII), amount of daily and maximum 5-day precipitation (RX1day and RX5day) similar to Vincent *et al.* (2011) for the Western Indian Ocean and Aguilar *et al.* (2009) for Guinea and Central Africa. This reduction was most obvious in the east coast area and agreed with Tadross *et al.* (2008). The regional trend of PRCPTOT was about 0.56%/decade smaller from 1950 to 2018 than in Vincent *et al.* (2011). On the contrary, some authors observed an increase in total precipitation accompanied by an increased simple daily precipitation index, heavy precipitation, daily precipitation and maximum 5-day precipitation for Global (Alexander *et al.*, 2006 and Dunn *et al.*, 2020), Central America and northern South America (Aguilar *et al.*, 2005), Zimbabwe (Aguilar *et al.*, 2009) and West Africa (Barry *et al.* 2018). Moreover, New *et al.* (2006) found a reduction in total precipitation, but daily rainfall intensity significantly increased for South and West Africa. Our study detected a shift in the magnitude of precipitation (i.e., a decrease in the number of precipitation events causes a reduction in the amount of rainfall) which was more tangible in the 2000–2018 period of intensified drying (in agreement with more than 60% of stations). This period was prone to extreme drought events (i.e., intensity greater than 2). Their magnitude and duration increased from 1950 to 2018. This result was ascertained by Kogan and Guo (2016), and Masih *et al.* (2014) noted severe and extreme drought events in the 21st century globally and in Africa, respectively. A

fact that may be related to the long drought in Australia called the 'Big dry' (Ummenhofer *et al.*, 2009 and Heberger, 2012) which ran from 1997 to 2010.

Madagascar houses endemic fauna and flora (Goodman and Benstead, 2005; Raven *et al.*, 2020), and such changes in temperature and precipitation threaten this biodiversity. For instance, Raxworthy *et al.* (2008) observed an upslope displacement of 30 species in the Tsaratanana Massif in northern Madagascar due to warming trends. Moreover, we showed that, if drought magnitude and duration increased, then the effects of drought could be seen in the environmental system, as pointed out by Vicente-Serrano *et al.* (2020). For instance, Sato *et al.* (2014) observed that lemurs altered their diets to cope with environmental stress due to changes in temperature and rainfall patterns. In addition, these changes affect socioeconomic sectors in Madagascar. Harvey *et al.* (2014) indicated the effects of climate change for smallholder farmers and Nematchoua (2019) outlined the increasing demand for cooling energy. Our findings contribute to implementing adaptation and mitigation strategies to cope with such threats in Madagascar. For instance, articles on climate change adaptation (e.g., Hannah *et al.*, 2008; Busch *et al.*, 2012) and on climate change mitigation (e.g., Nogueira *et al.*, 2020) may be updated.

This paper reveals new features in changes (e.g., appearance of very extreme cold nights and warm days, a shift in precipitation magnitude and ever-increasing consecutive drought events) in the climate of Madagascar. The next step in this research is to delve further into an analysis of the findings by continuous improvement in the data set through Data Rescue (DARE) and homogenization, in order to reduce uncertainty (Skrynyk *et al.*, 2021). For example, elements (e.g., solar radiation, wind speed, etc.) should be added to use a more robust estimation of reference evapotranspiration (Beguería *et al.*, 2014). Future key questions are: are model outputs from CMIP5, CMIP6 or CORDEX consistent with our observational trends? And do our observational trends relate to certain atmospheric mechanisms?

6 | CONCLUSION

This paper used state-of-the-art daily data quality control and homogenization processes to guarantee robustness in climate data records before assessing climate trends. It also gave a broader range of climate indices to update knowledge on climate change in Madagascar. Our findings were most significant at 0.05 level for temperature indices at regional and station level. The temporal evolution of our regional temperature indices followed the warming. At station level, all stations

(100%) indicated significant positive trends for means of annual temperatures and 74% presented negative DTR trends. For temperature extremes, night-time indices were higher than daytime indicators. Most precipitation indices had negative trends, and total precipitation (PRCPTOT) decreased (significant at 0.05 level) for regions, but at station level significant negative trends were 29.6 and 7.4%, and non-significant ones were 55.6 and 63.0% from 1950 to 2018 and 2000 to 2018, respectively. Regional time series also showed a shift in precipitation magnitude, which caused intensified drying after 2000 for all indicators. Drought indices highlighted an increased number of drought events after the 1980s.

ACKNOWLEDGEMENTS

This study could not have been carried out without financial support from the INDECIS project, which is a part of ERA4CS, an ERA-NET initiated by JPI Climate, and funded by FORMAS (SE), DLR (DE), BMWFW (AT), IFD (DK), MINECO (ES), ANR (FR) with co-funding by the European Union (Grant 690462), and without the climate data from the Directorate General of Meteorology (DGM) of Madagascar. The authors thank anonymous reviewers for their in-depth reading of the manuscript and the valuable comments and suggestions they have made.

AUTHOR CONTRIBUTIONS

Enric Aguilar: Conceptualization; formal analysis; funding acquisition; methodology; project administration; resources; software; supervision; validation; writing-original draft; writing-review & editing. **Oleg Skrynyk:** Data curation; methodology; resources; software; validation; writing-review & editing. **Sergio Vicente-Serrano:** Methodology; resources; software; validation; writing-review & editing. **F Domínguez-Castro:** Resources; software; validation; writing-review & editing.

ORCID

Luc Yannick Andréas Randriamarolaza  <https://orcid.org/0000-0002-2939-2250>

Enric Aguilar  <https://orcid.org/0000-0002-8384-377X>

Oleg Skrynyk  <https://orcid.org/0000-0001-8827-0280>

Sergio M. Vicente-Serrano  <https://orcid.org/0000-0003-2892-518X>

Fernando Domínguez-Castro  <https://orcid.org/0000-0003-3085-7040>

REFERENCES

- Abatan, A.A., Abiodun, B.J., Lawal, K.A. and Gutowski, W.J. (2016) Trends in extreme temperature over Nigeria from percentile-based threshold indices. *International Journal of Climatology*, 36(6), 2527–2540. <https://doi.org/10.1002/joc.4510>.

- Abrha, H. and Hagos, H. (2019) Future drought and aridity monitoring using multi-model approach under climate change in Hintalo Wejerat district, Ethiopia. *Sustainable Water Resources Management*, 5(4), 1963–1972. <https://doi.org/10.1007/s40899-019-00350-1>.
- Aguilar, E., Auer, I., Brunet, M., Peterson, T.C. and Wieringa, J. (2003) *WMO Guidelines on Climate Metadata and Homogenization*. WCDMP no.53, WMO-TD No. 1186. Geneva, Switzerland: WMO.
- Aguilar, E., Aziz Barry, A., Brunet, M., Ekang, L., Fernandes, A., Massoukina, M., Mbah, J., Mhanda, A., do Nascimento, D.J., Peterson, T.C., Thamba Umba, O., Tomou, M. and Zhang, X. (2009) Changes in temperature and precipitation extremes in western Central Africa, Guinea Conakry, and Zimbabwe, 1955–2006. *Journal of Geophysical Research-Atmospheres*, 114(2), D02115. <https://doi.org/10.1029/2008JD011010>.
- Aguilar, E., Peterson, T.C., Ramírez Obando, P., Frutos, R., Retana, J.A., Solera, M., Soley, J., González García, I., Araujo, R.M., Rosa Santos, A., Valle, V.E., Brunet, M., Aguilar, L., Álvarez, L., Bautista, M., Castañón, C., Herrera, L., Ruano, E., Sinay, J.J., Sánchez, E., Hernández Oviedo, G.I., Obed, F., Salgado, J.E., Vázquez, J.L., Baca, M., Gutiérrez, M., Centella, C., Espinosa, J., Martínez, D., Olmedo, B., Ojeda Espinoza, C.E., Núñez, R., Haylock, M., Benavides, H. and Mayorga, R. (2005) Changes in precipitation and temperature extremes in Central America and northern South America, 1961–2003. *Journal of Geophysical Research-Atmospheres*, 110(23), D23107. <https://doi.org/10.1029/2005JD006119>.
- Alexander, L.V., Zhang, X., Peterson, T.C., Caesar, J., Gleason, B., Klein Tank, A.M.G., Haylock, M., Collins, D., Trewin, B., Rahimzadeh, F., Tagipour, A., Rupa Kumar, K., Revadekar, J., Griffiths, G., Vincent, L., Stephenson, D.B., Burn, J., Aguilar, E., Brunet, M., Taylor, M., New, M., Zhai, P., Rusticucci, M. and Vazquez-Aguirre, L. (2006) Global observed changes in daily climate extremes of temperature and precipitation. *Journal of Geophysical Research-Atmospheres*, 111(5), D05109. <https://doi.org/10.1029/2005JD006290>.
- Alexandersson, H. (1986) A homogeneity test applied to precipitation data. *Journal of Climatology*, 6(6), 661–675. <https://doi.org/10.1002/joc.3370060607>.
- Alexandersson, H. and Moberg, A. (1997) Homogenization of Swedish temperature data. Part I: homogeneity test for linear trends. *International Journal of Climatology*, 17(1), 25–34. [https://doi.org/10.1002/\(SICI\)1097-0088\(199701\)17:1<25::AID-JOC103>3.0.CO;2-J](https://doi.org/10.1002/(SICI)1097-0088(199701)17:1<25::AID-JOC103>3.0.CO;2-J).
- Barimalala, R., Blamey, R.C., Desbiolles, F. and Reason, C.J.C. (2020) Variability in the Mozambique Channel trough and impacts on southeast African rainfall. *Journal of Climate*, 33(2), 749–765. <https://doi.org/10.1175/JCLI-D-19-0267.1>.
- Barry, A.A., Caesar, J., Klein Tank, A.M.G., Aguilar, E., McSweeney, C., Cyrille, A.M., Nikiema, M.P., Narcisse, K.B., Sima, F., Stafford, G., Touray, L.M., Ayilari-Naa, J.A., Mendes, C.L., Tounkara, M., Gar-Glahn, E.V.S., Coulibaly, M. S., Dieh, M.F., Mouhaimouni, M., Oyegade, J., Sambou, E. and Laogbessi, E.T. (2018) West Africa climate extremes and climate change indices. *International Journal of Climatology*, 38, e921–e938. <https://doi.org/10.1002/joc.5420>.
- Beguiería, S., Vicente-Serrano, S.M., Reig, F. and Latorre, B. (2014) Standardized precipitation evapotranspiration index (SPEI) revisited: parameter fitting, evapotranspiration models, tools, datasets and drought monitoring. *International Journal of Climatology*, 34(10), 3001–3023. <https://doi.org/10.1002/joc.3887>.
- Besselaar, E.J.M., Klein Tank, A.M.G., Schrier, G. and Jones, P.D. (2012) Synoptic messages to extend climate data records. *Journal of Geophysical Research. Atmospheres*, 117(7), D07101. <https://doi.org/10.1029/2011JD016687>.
- Bronaugh, D. and Werner, A. (2019) zyp: Zhang+Yue-Pilon Trends Package. R package version 0.10–1.1 Available at: <https://cran.r-project.org/web/packages/zyp/index.html> [Accessed 25th January 2019]
- Busch, J., Dave, R., Hannah, L., Cameron, A., Rasolohery, A., Roehrdanz, P. and Schatz, G. (2012) Climate change and the cost of conserving species in Madagascar. *Conservation Biology*, 26(3), 1–48. <https://doi.org/10.1111/j.1523-1739.2012.01838.x>.
- Byrd, K.B., Lorenz, A.A., Anderson, J.A., Wallace, C.S.A., Moore-O’Leary, K.A., Isola, J., Ortega, R. and Reiter, M.E. (2020) Quantifying drought’s influence on moist soil seed vegetation in California’s Central Valley through remote sensing. *Ecological Applications*, 30, e02153. <https://doi.org/10.1002/eap.2153>.
- Domínguez-Castro, F., Reig, F., Vicente-Serrano, S.M., Aguilar, E., Peña-Angulo, D., Noguera, I., Revuelto, J., van der Schrier, G. and El Kenawy, A.M. (2020) A multidecadal assessment of climate indices over Europe. *Scientific Data*, 7(1), 125. <https://doi.org/10.1038/s41597-020-0464-0>.
- Domínguez-Castro, F., Vicente-Serrano, S.M., Tomás-Burguera, M., Peña-Gallardo, M., Beguería, S., El Kenawy, A., Luna, Y. and Morata, A. (2019) High-spatial-resolution probability maps of drought duration and magnitude across Spain. *Natural Hazards and Earth System Sciences*, 19(3), 611–628. <https://doi.org/10.5194/nhess-19-611-2019>.
- Donque, G. (1972) The climatology of Madagascar. In: Battistini, R. and Richard-Vindard, G. (Eds.) *Biogeography and Ecology in Madagascar. Monographiae Biologicae*, Vol. 21. Dordrecht: Springer. https://doi.org/10.1007/978-94-015-7159-3_3.
- Dunn, R.J.H., Alexander, L.V., Donat, M.G., Zhang, X., Bador, M., Herold, N., Lippmann, T., Allan, R., Aguilar, E., Barry, A.A., Brunet, M., Caesar, J., Chagnaud, G., Cheng, V., Cinco, T., Durre, I., de Guzman, R., Htay, T.M., Ibadullah, W.M.W., Ibrahim, M.K.I.B., Khoshkam, M., Kruger, A., Kubota, H., Leng, T.W., Lim, G., Li-Sha, L., Marengo, J., Mbatha, S., McGree, S., Menne, M., de los Milagros Skansi, M., Ngwenya, S., Nkrumah, F., Oonariya, C., Pabon-Caicedo, J.D., Panthou, G., Pham, C., Rahimzadeh, F., Ramos, A., Salgado, E., Salinger, J., Sané, Y., Sopaheluwakan, A., Srivastava, A., Sun, Y., Timbal, B., Trachow, N., Trewin, B., van der Schrier, G., Vazquez-Aguirre, J., Vasquez, R., Villarroel, C., Vincent, L., Vischel, T., Vose, R. and Yussuf, M.N.A.B.H. (2020) Development of an updated global land in-situ-based dataset of temperature and precipitation extremes: HadEX3. *Journal of Geophysical Research. Atmospheres*, 125, e2019JD032263. <https://doi.org/10.1029/2019JD032263>.
- Easterling, D.R., Alexander, L.V., Mokssit, A. and Detemmerman, V. (2003) CCI/CLIVAR workshop to develop priority climate indices. *Bulletin of the American Meteorological Society*, 84(10), 1403–1407. <https://doi.org/10.1175/BAMS-84-10-1403>.
- Goodman, S.M. and Benstead, J.P. (2005) Updated estimates of biotic diversity and endemism for Madagascar. *Oryx*, 39(1), 73–77. <https://doi.org/10.1017/S0030605305000128>.

- Guijarro, J.A. (2018) Homogenization of climatic series with Climatol. Version 3.1.1. Guide.
- Guijarro, J.A., Aguilar, E., Caloiero, T., Coscarelli, R., Curley, M. and Pérez-Zanón N (2018): Homogenization of daily Essential Climatic Variables with Climatol 3.1 within the INDECIS project. EMS Annual Meeting (Budapest, 3–7 September)
- Guijarro, J.A., Aguilar, E., Sigró, J., Stépanek, P., Venema, V. and Zahradníček, P. (2019): Benchmarking results of the homogenization of daily Essential Climatic Variables within the INDECIS project. Oral at EGU General Assembly (Vienna, 7–12 April)
- Hannah, L., Dave, R., Lowry, P.P., Andelman, S., Andrianarisata, M., Andriamaro, L., Cameron, A., Hijmans, R., Kremen, C., MacKinnon, J., Randrianasolo, H.H., Andriambololonera, S., Razafimpahanana, A., Randriamahazo, H., Randrianarisoa, J., Razafinjatovo, P., Raxworthy, C., Schatz, G.E., Tadross, M. and Wilmé, L. (2008) Climate change adaptation for conservation in Madagascar. *Biology Letters*, 4(5), 590–594. <https://doi.org/10.1098/rsbl.2008.0270>.
- Hargreaves, G.H. (1994) Defining and using reference evapotranspiration. *Journal of Irrigation and Drainage Engineering*, 120(6), 1132–1139. [http://doi.org/10.1061/\(ASCE\)0733-9437\(1994\)120:6\(1132\)](http://doi.org/10.1061/(ASCE)0733-9437(1994)120:6(1132)).
- Harvey, C.A., Rakotobe, Z.L., Rao, N.S., Dave, R., Razafimahatratra, H., Rabarijohn, R.H., Rajaofara, H. and MacKinnon, J.L. (2014) Extreme vulnerability of smallholder farmers to agricultural risks and climate change in Madagascar. *Philosophical Transactions of the Royal Society, B: Biological Sciences*, 369(1639), 20130089. <https://doi.org/10.1098/rstb.2013.0089>.
- Heberger, M. (2012) Australia's millennium drought: impacts and responses. In: Gleick, P.H. (Ed.) *The World's Water Volume 7: The Biennial Report on Freshwater 97* © 2012 Pacific Institute for Studies in Development, Environment, and Security Resources. Island Press, Washington, DC: The World's Water. https://doi.org/10.5822/978-1-59726-228-6_5.
- Hoegh-Guldberg, O., Jacob, D., Taylor, M., Bindi, M., Brown, S., Camilloni, I., Diedhiou, A., Djalante, R., Ebi, K.L., Engelbrecht, F., Guiot, J., Hijioka, Y., Mehrotra, S., Payne, A., Seneviratne, S.I., Thomas, A., Warren, R. and Zhou, G. (2018) Impacts of 1.5°C global warming on natural and human systems. In: Masson-Delmotte, V., Zhai, P., Pörtner, H.-O., Roberts, D., Skea, J., Shukla, P.R., Pirani, A., Moufouma-Okia, W., Péan, C., Pidcock, R., Connors, S., Matthews, J.B.R., Chen, Y., Zhou, X., Gomis, M.I., Lonnoy, E., Maycock, T., Tignor, M. and Waterfield, T. (Eds.) Available at *Global Warming of 1.5°C. An IPCC Special Report on the Impacts of Global Warming of 1.5°C above Pre-Industrial Levels and Related Global Greenhouse Gas Emission Pathways, in the Context of Strengthening the Global Response to the Threat of Climate Change, Sustainable Development, and Efforts to Eradicate Poverty*. Geneva, Switzerland: World Meteorological Organization Technical Document, <https://www.ipcc.ch/sr15> [Accessed May 25, 2020].
- Hunziker, S., Gubler, S., Calle, J., Moreno, I., Andrade, M., Velarde, F., Ticona, L., Carrasco, G., Castellón, Y., Oria, C., Croci-Maspoli, M., Konzelmann, T., Rohrer, M. and Brönnimann, S. (2017) Identifying, attributing, and overcoming common data quality issues of manned station observations. *International Journal of Climatology*, 37(11), 4131–4145. <https://doi.org/10.1002/joc.5037>.
- Jarvis, A., Reuter, H.I. Nelson, A. and Guevara, E. (2008) Hole-filled SRTM for the Globe Version 4, from the CGIAR-CSI SRTM 90m Database. Available at: <http://srtm.csi.cgiar.org>. [Accessed April 20, 2020].
- Jessica, M.B., Subrahmanyam, B., Nyadjro, E.S. and Murty, V.S.N. (2016) Tropical cyclone activity over the southwest tropical Indian Ocean. *Journal of Geophysical Research, Oceans*, 121(9), 6762–6778. <https://doi.org/10.1002/2016JC011992>.
- Jury, M.R., Parker, B. and Waliser, D. (1994) Evolution and variability of the ITCZ in the SW Indian Ocean: 1988–90. *Theoretical and Applied Climatology*, 48(4), 187–194. <https://doi.org/10.1007/BF00867048>.
- Keshitgar, B., Alizadeh-Choobari, O. and Irannejad, P. (2020) Seasonal and interannual variations of the Intertropical convergence zone over the Indian Ocean based on an energetic perspective. *Climate Dynamics*, 54(7–8), 3627–3639. <https://doi.org/10.1007/s00382-020-05195-5>.
- Kogan, F. and Guo, W. (2016) Early twenty-first-century droughts during the warmest climate. *Geomatics, Natural Hazards and Risk*, 7(1), 127–137. <https://doi.org/10.1080/19475705.2013.878399>.
- Kruger, A.C. and Nxumalo, M. (2017) Surface temperature trends from homogenized time series in South Africa: 1931–2015. *International Journal of Climatology*, 37(5), 2364–2377. <https://doi.org/10.1002/joc.4851>.
- Leroux, M.D., Meister, J., Mekies, D., Dorla, A.L. and Caroff, P. (2018) A climatology of Southwest Indian Ocean tropical systems: their number, tracks, impacts, sizes, empirical maximum potential intensity, and intensity changes. *Journal of Applied Meteorology and Climatology*, 57(4), 1021–1041. <https://doi.org/10.1175/JAMC-D-17-0094.1>.
- Macron, C., Richard, Y., Garot, T., Bessafi, M., Pohl, B., Ratiarison, A. and Razafindrabe, A. (2016) Intraseasonal rainfall variability over Madagascar. *Monthly Weather Review*, 144(5), 1877–1885. <https://doi.org/10.1175/MWR-D-15-0077.1>.
- Masih, I., Maskey, S., Mussá, F.E.F. and Trambauer, P. (2014) A review of droughts on the African continent: a geospatial and long-term perspective. *Hydrology and Earth System Sciences*, 18(9), 3635–3649. <https://doi.org/10.5194/hess-18-3635-2014>.
- Matyas, C.J. (2015) Tropical cyclone formation and motion in the Mozambique Channel. *International Journal of Climatology*, 35(3), 375–390. <https://doi.org/10.1002/joc.3985>.
- Mestre, O., Domonkos, P., Picard, F., Auer, I., Robin, S., Lebarbier, E., Böhm, R., Aguilar, E., Guijarro, J., Vertachnik, G., Klancar, M., Dubuisson, B. and Stepanek, P. (2013) HOMER: a homogenization software – methods and applications. *IDOJARAS - Quarterly Journal of the Hungarian Meteorological Service*, 117(1), 47–67.
- Moberg, A. and Alexandersson, H. (1997) Homogenization of Swedish temperature data. Part II: homogenized gridded air temperature compared with a subset of global gridded air temperature since 1861. *International Journal of Climatology*, 17, 35–54. [https://doi.org/10.1002/\(SICI\)1097-0088\(199701\)17:1<35::AID-JOC104>3.0.CO;2-F](https://doi.org/10.1002/(SICI)1097-0088(199701)17:1<35::AID-JOC104>3.0.CO;2-F).
- Morid, S., Smakhtin, V. and Moghaddasi, M. (2006) Comparison of seven meteorological indices for drought monitoring in Iran. *International Journal of Climatology*, 26(7), 971–985. <https://doi.org/10.1002/joc.1264>.

- Nematchoua, M.K. (2019) A study of climate change and energy consumption in Madagascar Island. *Health and Environment*, 1 (1), 9–27. <https://doi.org/10.25082/he.2019.01.002>.
- Nematchoua, M.K., Ricciardi, P., Orosa, J.A. and Buratti, C. (2018) A detailed study of climate change and some vulnerabilities in Indian Ocean: a case of Madagascar Island. *Sustainable Cities and Society*, 41, 886–898. <https://doi.org/10.1016/j.scs.2018.05.040>.
- New, M., Hewitson, B., Stephenson, D.B., Tsiga, A., Kruger, A., Manhique, A., Gomez, B., Coelho, C.A.S., Masisi, D.N., Kululanga, E., Mbambalala, E., Adesina, F., Saleh, H., Kanyanga, J., Adosi, J., Bulane, L., Fortunata, L., Mdoka, M.L. and Lajoie, R. (2006) Evidence of trends in daily climate extremes over southern and West Africa. *Journal of Geophysical Research-Atmospheres*, 111(14), 1–11. <https://doi.org/10.1029/2005JD006289>.
- Niang, I., Ruppel, O.C., Abdrabo, M.A., Essel, A., Lennard, C., Padgham, J. and Urquhart, P. (2015) Africa. In: Barros, V.R., Field, C.B., Dokken, D.J., Mastrandrea, M.D., Mach, K.J., Bilir, T.E., Chatterjee, M., Ebi, K.L., Estrada, Y.O., Genova, R. C., Girma, B., Kissel, E.S., Levy, A.N., MacCracken, S., Mastrandrea, P.R. and White, L.L. (Eds.) *Climate Change 2014: Impacts, Adaptation and Vulnerability: Part B: Regional Aspects: Working Group II Contribution to the Fifth Assessment Report of the Intergovernmental Panel on Climate Change*. Cam: Cambridge University Press, pp. 1199–1266. <https://doi.org/10.1017/CBO9781107415386.002>.
- Nogueira, L.P., Longa, F.D. and van der Zwaan, B. (2020) A cross-sectoral integrated assessment of alternatives for climate mitigation in Madagascar. *Climate Policy*, 20, 1257–1273. <https://doi.org/10.1080/14693062.2020.1791030>.
- Pérez-Zanón, N., Sigró, J., Aguilar, E., Guijarro, J.A., van der Schrier, G., Stepanek, P., Zahradnicek, P., Coscarelli, R., Engström, E., Curley, M., Caloiero, T., Lledó, L., Ramon, J., Valente, M.A. and Carvalho, S. (2018): First steps towards a benchmarking experiment in quality control and homogenization of observed data. EMS Annual Meeting (Budapest, 3-7 September)
- Peterson, T.C., Easterling, D.R., Karl, T.R., Groisman, P., Nicholls, N., Plummer, N., Torok, S., Auer, I., Boehm, R., Gullett, D., Vincent, L., Heino, R., Tuomenvirta, H., Mestre, O., Szentimrey, T., Salinger, J., Førland, E.J., Hanssen-Bauer, I., Alexandersson, H., Jones, P. and Parker, D. (1998) Homogeneity adjustments of *in situ* atmospheric climate data: a review. *International Journal of Climatology*, 18(13), 1493–1517. [https://doi.org/10.1002/\(SICI\)1097-0088\(19981115\)18:13<1493::AID-JOC329>3.0.CO;2-T](https://doi.org/10.1002/(SICI)1097-0088(19981115)18:13<1493::AID-JOC329>3.0.CO;2-T).
- Randriamahefasoa, T.S.M. and Reason, C.J.C. (2017) Interannual variability of rainfall characteristics over southwestern Madagascar. *Theoretical and Applied Climatology*, 128(1–2), 421–437. <https://doi.org/10.1007/s00704-015-1719-0>.
- Ratna, S.B., Behera, S., Ratnam, J.V., Takahashi, K. and Yamagata, T. (2013) An index for tropical temperate troughs over southern Africa. *Climate Dynamics*, 41(2), 421–441. <https://doi.org/10.1007/s00382-012-1540-8>.
- Raven, P.H., Gereau, R.E., Phillipson, P.B., Chatelain, C., Jenkins, C.N. and Ulloa, C.U. (2020) The distribution of biodiversity richness in the tropics. *Science Advances*, 6(37), eabc6228. <https://doi.org/10.1126/sciadv.abc6228>.
- Raxworthy, C.J., Pearson, R.G., Rabibisoa, N., Rakotondrazafy, A. M., Ramanamanjato, J.B., Raselimanana, A.P., Wu, S., Nussbaum, R.A. and Stone, D.A. (2008) Extinction vulnerability of tropical montane endemism from warming and upslope displacement: a preliminary appraisal for the highest massif in Madagascar. *Global Change Biology*, 14(8), 1703–1720. <https://doi.org/10.1111/j.1365-2486.2008.01596.x>.
- Sato, H., Ichino, S. and Hanya, G. (2014) Dietary modification by common brown lemurs (*Eulemur fulvus*) during seasonal drought conditions in western Madagascar. *Primates*, 55(2), 219–230. <https://doi.org/10.1007/s10329-013-0392-0>.
- Sen, P.K. (1968) Estimates of the regression coefficient based on Kendall's tau. *Journal of the American Statistical Association*, 63 (324), 1379–1389. <https://doi.org/10.1080/01621459.1968.10480934>.
- Skrynyk, O., Aguilar, E., Guijarro, J., Randriamarolaza, L.Y.A. and Bubin, S. (2021) Uncertainty evaluation of Climatol's adjustment algorithm applied to daily air temperature time series. *International Journal of Climatology*, 41(Suppl. 1), E2395–E2419. <https://doi.org/10.1002/joc.6854>.
- Squintu, A.A., van der Schrier, G., Štěpánek, P., Zahradníček, P. and Tank, A.K. (2020) Comparison of homogenization methods for daily temperature series against an observation-based benchmark dataset. *Theoretical and Applied Climatology*, 140 (1–2), 285–301. <https://doi.org/10.1007/s00704-019-03018-0>.
- Tadross, M., Randriamarolaza, L., Rabefitia, Z. and Yip, Z.K. (2008) *Climate Change in Madagascar: Recent, Past and Future*. Washington, DC: World Bank.
- Tara James, C. and Stacia, Y. (2014) Climate change adaptation in the Southwest Indian Ocean: case study of the perception of risk, common coping strategies and the potential for micro-insurance. *Journal of Geography & Natural Disasters*, 04 (02), 2–9. <https://doi.org/10.4172/2167-0587.1000129>.
- Trewin, B. (2010) Exposure, instrumentation, and observing practice effects on land temperature measurements. *WIREs Climate Change*, 1(4), 490–506. <https://doi.org/10.1002/wcc.46>.
- Ummenhofer, C.C., England, M.H., McIntosh, P.C., Meyers, G.A., Pook, M.J., Risbey, J.S., Gupta, A.S. and Taschetto, A.S. (2009) What causes Southeast Australia's worst droughts? *Geophysical Research Letters*, 36(4), L04706. <https://doi.org/10.1029/2008GL036801>.
- Venema, V., Mestre, O., Aguilar, E., Auer, I., Guijarro, J.A., Domonkos, P., Vertacnik, G., Szentimrey, T., Stepanek, P., Zahradnicek, P., Viarre, J., Muller-Westermeier, G., Lakatos, M., Williams, C.N., Menne, M., Lindau, R., Rasol, D., Rustemeier, E., Kolokythas, K., Marinova, T., Andresen, L., Acquotta, F., Fratianni, S., Cheval, S., Klancar, M., Brunetti, M., Gruber, C., Duran, M.P., Likso, T., Esteban, P. and Brandsma, T. (2012) Benchmarking monthly homogenization algorithms. *Climate of the Past*, 8, 89–115. <https://doi.org/10.5194/cp-8-89-2012>.
- Vicente-Serrano, S.M., Beguería, S. and López-Moreno, J.I. (2010) A multiscalar drought index sensitive to global warming: the standardized precipitation evapotranspiration index. *Journal of Climate*, 23(7), 1696–1718. <https://doi.org/10.1175/2009JCLI2909.1>.
- Vicente-Serrano, S.M., Quiring, S.M., Peña-Gallardo, M., Yuan, S. and Domínguez-Castro, F. (2020) A review of environmental droughts: increased risk under global warming? *Earth-Science Reviews*, 201, 102953. <https://doi.org/10.1016/j.earscirev.2019.102953>.
- Vincent, L.A., Aguilar, E., Saindou, M., Hassane, A.F., Jumaux, G., Roy, D., Booneady, P., Virasmi, R.,

- Randriamarolaza, L.Y.A., Faniriantsoa, F.R., Amelie, V., Seeward, H. and Montfraix, B. (2011) Observed trends in indices of daily and extreme temperature and precipitation for the countries of the western Indian Ocean, 1961-2008. *Journal of Geophysical Research-Atmospheres*, 116(10), 1–12. <https://doi.org/10.1029/2010JD015303>.
- Vincent, L.A., Zhang, X., Bonsal, B.R. and Hogg, W.D. (2002) Homogenization of daily temperatures over Canada. *Journal of Climate*, 15(11), 1322–1334. [https://doi.org/10.1175/1520-0442\(2002\)015<1322:HODTOC>2.0.CO;2](https://doi.org/10.1175/1520-0442(2002)015<1322:HODTOC>2.0.CO;2).
- Whan, K., Alexander, L.V., Imielska, A., Mcgree, S., Jones, D., Ene, E., Finaulahi, S., Inape, K., Jacklick, L., Kumar, R., Laurent, V., Malala, H., Malsale, P., Pulehetoa-Mitiepo, R., Ngemaes, M., Peltier, A., Porteous, A., Seuseu, S., Skilling, E., Tahani, L., Toorua, U. and Vaiimene, M. (2014) Trends and variability of temperature extremes in the tropical Western Pacific. *International Journal of Climatology*, 34(8), 2585–2603. <https://doi.org/10.1002/joc.3861>.
- World Meteorological Organization (WMO), 2020: Guidelines on Homogenization (WMO-No. 1245). Geneva.
- Xu, W., Li, Q., Wang, X.L., Yang, S., Cao, L. and Feng, Y. (2013) Homogenization of Chinese daily surface air temperatures and analysis of trends in the extreme temperature indices. *Journal of Geophysical Research-Atmospheres*, 118(17), 9708–9720. <https://doi.org/10.1002/jgrd.50791>.
- Yosef, Y., Aguilar, E. and Alpert, P. (2019) Changes in extreme temperature and precipitation indices: using an innovative daily homogenized database in Israel. *International Journal of Climatology*, 39(13), 5022–5045. <https://doi.org/10.1002/joc.6125>.
- Yosef, Y., Aguilar, E. and Alpert, P. (2021) Is it possible to fit extreme climate change indices together seamlessly in the era of accelerated warming? *The International Journal of Climatology*, 41(S1), E952–E963. <https://doi.org/10.1002/joc.6740>.
- Zhang, X., Alexander, L., Hegerl, G.C., Jones, P., Tank, A.K., Peterson, T.C., Trewin, B. and Zwiers, F.W. (2011) Indices for monitoring changes in extremes based on daily temperature and precipitation data. *WIREs Climate Change*, 2, 851–870. <https://doi.org/10.1002/wcc.147>.
- Zhang, X., Vincent, L.A., Hogg, W.D. and Niitsoo, A. (2000) Temperature and precipitation trends in Canada during the 20th century. *Atmosphere-Ocean*, 38(3), 395–429. <https://doi.org/10.1080/07055900.2000.9649654>.

How to cite this article: Randriamarolaza, L. Y. A., Aguilar, E., Skrynyk, O., Vicente-Serrano, S. M., & Domínguez-Castro, F. (2021). Indices for daily temperature and precipitation in Madagascar, based on quality-controlled and homogenized data, 1950–2018. *International Journal of Climatology*, 1–24. <https://doi.org/10.1002/joc.7243>